***These*** **a** ***post-peer-review, pre-copyedit version of an article published in the Journal of Building Engineering. The final authenticated version is available online at: https://doi.org/10.1016/j.jobe.2021.103061***

# Seismic Risk Assessment and Intervention Prioritization for Italian Medieval Churches

David Pirchio[a]*, Kevin Q. Walsh[a,b], Elizabeth Kerr[a], Ivan Giongo[c], Marta Giaretton[d], Brad D. Weldon[e,b], Luca Ciocci[f], and Luigi Sorrentino[g]

*[a]Department of Civil and Environmental Engineering & Earth Sciences, University of Notre Dame, South Bend, Indiana, USA; [b]Frost Engineering & Consulting, Mishawaka, Indiana, USA; [c]Department of Civil, Environmental and Mechanical Engineering, University of Trento, Trento, Italy; [d]Dizhur Consulting, Auckland, New Zealand;; [e]Department of Civil Engineering, New Mexico State University, Las Cruces, New Mexico, USA; [f]Office for Cultural Heritage and Religious Buildings of the Diocese of Anagni-Alatri, Italy, [g]Department of Structural and Geotechnical Engineering, Sapienza University of Rome, Roma, Italy*

*e-mail: dpirchio@nd.edu; mail: Department of Civil and Environmental Engineering & Earth Sciences, University of Notre Dame, 156 Fitzpatrick Hall of Engineering, Notre Dame, IN 46556, USA

# Seismic Risk Assessment and Intervention Prioritization for Italian Medieval Churches

Rapid seismic risk assessments are critical to help practitioners, facility stakeholders, architectural heritage superintendence, and insurance companies in their asset management decision-making processes. In particular, the integrity of the Italian church portfolio has often been threatened by earthquakes. The Italian church portfolio includes thousands of religious buildings, representing pivotal facilities for the religious community, thus requiring an assessment methodology which accounts for the structural, architectural, cultural, and functional facets of churches. The methodology proposed herein combined both widely applied assessment techniques regarding structural vulnerability (e.g., “macro-blocks”) with a newly developed framework accounting for other important variables (e.g., the heritage significance of a church) to produce a rapid, quantifiable, and holistic approach to determine the relative seismic risk assessment of historic masonry churches. On-site surveys of 72 unreinforced masonry medieval churches across Italy were conducted. Following a hierarchical approach for the surveys, each risk component – hazard, vulnerability, exposure, and consequence – was defined throughout by the development of 13 different indices. Using the fuzzy set theory, the indices were aggregated into a final risk rating framework useful to provide stakeholders with a scientific-based prioritization list for the maintenance and strengthening intervention of their church portfolios.

Keywords: unreinforced masonry (URM) churches; risk components; seismic risk assessment; fuzzy set theory; property portfolio management; strengthening intervention prioritization.

## 1. Introduction

Churches retain a dominant importance among Italian cultural and spiritual life as they represent and contain a relevant component of Italian architectural and artistic heritage. However, this built heritage is subjected to significant risk due to earthquakes. During most of the major earthquakes in recent history in Italy, churches suffered damage and even partial or complete collapse [1, 2, 3]. Thus, it is desireable to prevent the structural failure of churches to avoid significant losses in terms of cultural heritage, reparation costs, and human lives. In these terms, the Italian church portfolio, with its immense architectural, cultural, and functional value, is the perfect case study for a proposed framework to holistically address facility risk as the function of several components (i.e., hazard, vulnerability, exposure, and consequences).

Several studies have been conducted regarding structural behavior, vulnerability assessment, and strengthening intervention on churches [1, 4]. Some of the historical research has focused on advanced modeling for single case studies (e.g., [5, 6]), while several observational studies were also conducted following strong earthquakes at a regional scale [1, 4, 7, 8, 9, 10, 11, 12]. Nationwide studies in other countries have been performed to predict the vulnerability of unreinforced masonry (URM) [13, 14]. However, all previous research (both in Italy and abroad) generally was limited to considering the seismic hazard and structural vulnerability of churches, mostly via the development of fragility curves [15, 16, 17, 18]. While fragility curves are the state-of-the-art technique for assessing the likelihood of collapse for URM churches, fragility curves offer no information regarding the inherent importance of the church itself, in terms of functionality, usage, economic and heritage value. The latter aspects are critical to portfolio-management decisions and to establish the prioritization of intervention among different churches based on a holistic risk analysis. The authors are not aware of any previous investigation of church seismic risk that encompass the Italian nationwide geographic footprint accounting holistically for all major components of risk.

## 2. Scope, Objectives, and Novelties

The dioceses often have limited budgets available to invest into strengthening interventions on existing buildings older than 20 years [19]. Therefore, prioritizing the detailed assessment and strengthening intervention across the church portfolio is a necessity for any diocese to best allocate limited resources.

To illustrate the developed methodology, 72 URM churches were assessed in nine different dioceses, distributed amongst six regions in North, Central and South Italy (Figure 1). The selected churches were surveyed for geometry, existing damage (i.e., cracking), and material properties to develop a suite of data for simulated models that may forecast possible collapse mechanisms. Some prototypical examples of the chosen churches are represented in Figure 2.

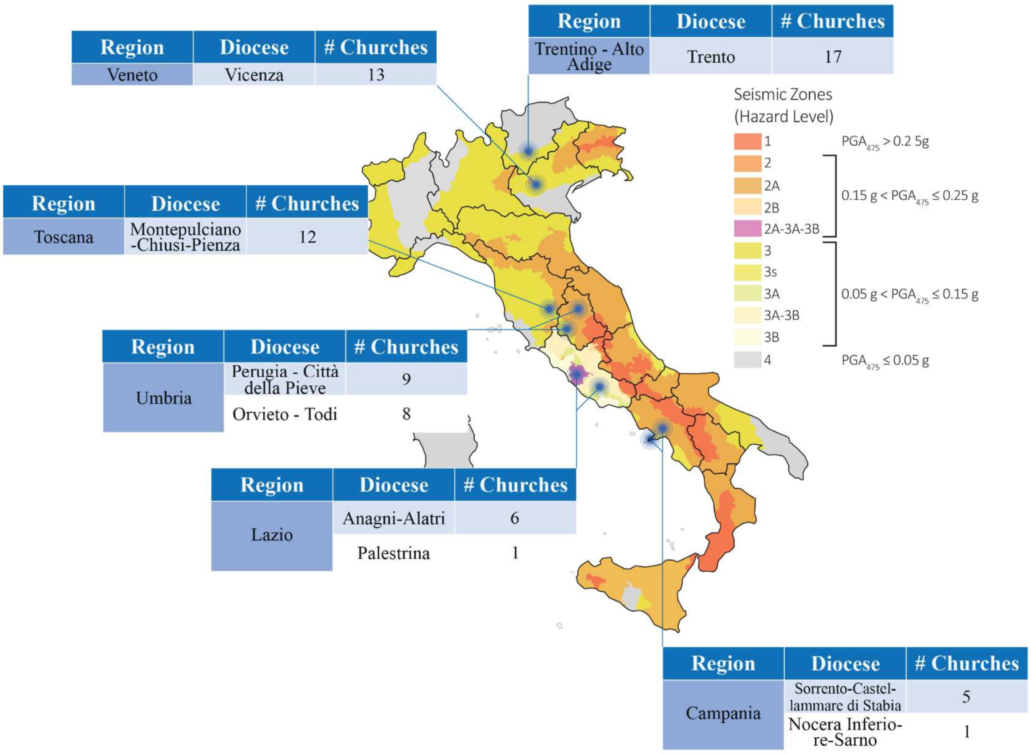


Figure 1 – Map of Italy indicating the nine dioceses in which churches were surveyed superimposed atop the national seismic hazard map. $PGA_{475}$ = peak ground acceleration for a 475-year average return period. Seismic zones adopted from the Italian National Civil Protection [20].


Figure 2 – Examples of prototypical churches surveyed: a) Santa Maria Assunta (Dasindo, Trentino – Alto Adige); b) San Matteo Apostolo (Cavazzale, Veneto); c) Santi Leonardo e Cristoforo (Monticchiello, Toscana); d) Sant Ansano Martire (Petrignano del Lago, Umbria); e) Maddalena (Alatri, Lazio); f) Santa Maria di Casarlano (Casarlano, Campania).

The goal of the research reported herein was to provide the church stakeholders and practitioners with a holistic and comprehensive seismic risk assessment methodology to be used as a scientific, objective basis in guiding the dioceses through their decision-making process for the allocation of maintenance and strengthening intervention funds. Established assessment techniques, when available, were applied to quantify the risk subcomponents (e.g., the macro-block vulnerability assessment per Italian Guidelines for the Assessment and the Reduction of the Seismic Risk of Cultural Heritage, or DPCM 9 February 2011 [21]). Novel efforts involved identifying and quantifying all the possible factors contributing to overall seismic risk, herein referred to as “risk subcomponents”, including non-structural issues. In total, thirteen different risk subcomponents were identified. While each risk subcomponent is addressed and described in later sections of the manuscript, the majority of these risk subcomponents are non-structural (e.g., the index of occupancy rate, and the index of community use). The relevance of non-structural aspects of risk assessment were observed by other authors [13, 22, 23], corresponding to previous efforts to develop criteria to evaluate risk components other than hazard and vulnerability. Nonetheless, these previous studies disregarded critical aspects (e.g., the actual usage of the building), and the criteria developed to assess the risk subcomponents were either too generic (e.g., importance level based on national codes for buildings), or without a clear scientific basis (e.g., occupancy limits to define the related exposure index were selected discretionally instead of based on statistical observations). In the current manuscript, the quantification of the non-structural risk subcomponents was based on a statistical analysis with other similar churches in regard to dimension and typology.

The risk subcomponents were quantified through the use of open access information and/or widely accepted metrics, and they were aggregated through the application of the "Fuzzy Set Theory" (FST), developed by Zadeh [24], resulting in a final relative risk rating for each church. While future research and advancements in the assessment of each risk subcomponent are desirable and encouraged, the authors' goal was to develop an applicable framework representing a state-of-the-art, holistic, and readily applied seismic risk assessment methodology for provisionally determining which churches warrant the allocation of resources for more sophisticated analysis and potential retrofitting.

## 3. Selection criteria

Churches chosen for consideration in this study were required to meet the following criteria:

- Various geographic locations (i.e., the researchers sought a range of geographic locations and seismicity zones);

- Active functionality within the community based on the church housing regular churchgoers, and the church's dominant role as a focal point of the spiritual life within the parish, given the relatively small sizes of the communities included in this study. This characteristic is represented by the term "community church";
- A construction period approximately between the years 1000 and 1500 (but occasionally slightly outside this timeframe); and
- A building planimetric layout preferably – but not exclusively – typical of stand-alone churches in city squares (i.e., piazzas).

Some of the information collected for each individual church can be found in Appendix A – Table A 1**Errore. L'origine riferimento non è stata trovata.Errore. L'origine riferimento non è stata trovata.**.

### ***3.1. Geographic Location***

To obtain a large variety of on-site conditions, the geographic location for the case studies of the current research was based on a representative range of seismicity, density of churches, climate and geologic/topographic environments, and cultural/historic background.

#### *3.1.1. Seismicity*

Churches were chosen so as to achieve a wide variety of locations across the spectrum of codified seismic hazards (Figure 1) to ensure the development of a generalizable assessment methodology. The diocese of Perugia-Città della Pieve in the Umbria region, the diocese of Anagni-Alatri in Lazio, and the diocese of Vicenza in Veneto are generally associated with higher seismicity compared to the other considered dioceses.

#### *3.1.2. Climate and Geologic/Topographic Conditions*

The distinctive climatic and geologic/topographic condition of each diocese plays an important role in the original choice of building materials. Churches surveyed in the current study were constructed using different techniques and materials, which represents a key variable for developing a generalizable risk assessment methodology. Thus, the range of surveyed dioceses (Figure 1) was also selected to account for the significant climatic and geologic/topographic differences between the various regions of the country:

- The diocese of Trento, in the region of Trentino – Alto Adige, is a mountainous area full of valleys within the Alps mountain range;
- The diocese of Vicenza, in the region of Veneto, occupies an ample part of the "Po Valley", the largest Italian plains region;
- The diocese of Montepulciano-Chiusi-Pienza, in the region of Toscana, is an area covered by steep hills;
- The dioceses of Perugia-Città della Pieve and Orvieto-Todi, in the region of Umbria, are hilly areas;
- The dioceses of Anagni-Alatri and Palestrina, in the region of Lazio, have churches that were constructed on steep hillsides near the Apennine mountains; and
- The dioceses of Sorrento-Castellammare di Stabia and Nocera Inferiore-Sarno, in the region of Campania, manage several churches located on sea cliffs and on hills close to the seaside.

### ***3.2. Active Functionality***

The churches were selected based on their role as a focal point in the spiritual life of the surrounding communities by identifying consecrated churches regularly utilized. In the context of the current research, the term “community churches” represents churches which are not primary cathedrals, in regard to size and fame, but are still actively visited and utilized by residents. The more famous cathedrals in Italy have often already been extensively assessed by others, and the stakeholders for cathedrals generally have access to more resources. In contrast, the “community churches” assessed in the current study have not often been extensively assessed by others. Finally, the architectural and cultural value of churches was considered in this phase as a discriminant. In selecting for assessment between two churches with similar functionality and occupancy rates, the church with a more qualitatively significant historical and heritage value was selected to be included in the study.

### *3.3. Original Construction Period*

Medieval churches were the primary focus of this research due to their prominent presence within Italy, their vulnerability as observed in past earthquakes, such as in Friuli-Venezia Giulia in 1976 [1], in Basilicata and Campania in 1980 [25], in Umbria-Marche in 1997 [4, 26], in L’Aquila in 2009 [2, 8, 27], and in central Italy in 2016 [11, 15]. Furthermore, medieval churches generally represent high levels of cultural and historic value, and they usually house invaluable artwork.

Churches chosen for assessment in the current study were generally constructed between the 11$^{th}$ and the 15$^{th}$ centuries, corresponding to the High and Late Middle Ages [28, 29]. This time period was chosen to achieve a greater homogeneity among sample churches in terms of construction techniques. Note that the timeframe refers to the original construction year, since many churches have been expanded and modified over time. Furthermore, churches originally constructed during the High and Late Middle Ages in Italy and still existing today are usually URM structures [30]. A few exceptions to the time period criteria for selection were made by assessing churches explicitly requested for survey by the dioceses, and some other churches that were typologically similar to medieval ones as shown in Appendix A – Table A 1.

### *3.4. Urban and Planimetric Layout*

The urban and planimetric layout of churches was also considered amongst the selection criteria, and churches were generally only selected for assessment if they were structurally isolated (i.e., stand-alone) from all neighboring buildings. The reason for focusing on structurally isolated churches is due to the greater simplicity and precision of quantifying all risk components of the church (especially vulnerability) as explicit from neighboring structures that may not even belong to the Church.  Furthermore, the interaction between adjacent buildings during an earthquake leads to highly variable predictions in structural models [31].

## 4. Church Typologies

The 72 selected churches surveyed as listed in Appendix A – Table A 1, were classified based on their general geometric attributes into various typological groupings as shown in Figure 3. Although a large variety of typologies was addressed in the current study, the single nave layout represented the majority of the analyzed cases, corresponding to 59.8% of the total number of churches.

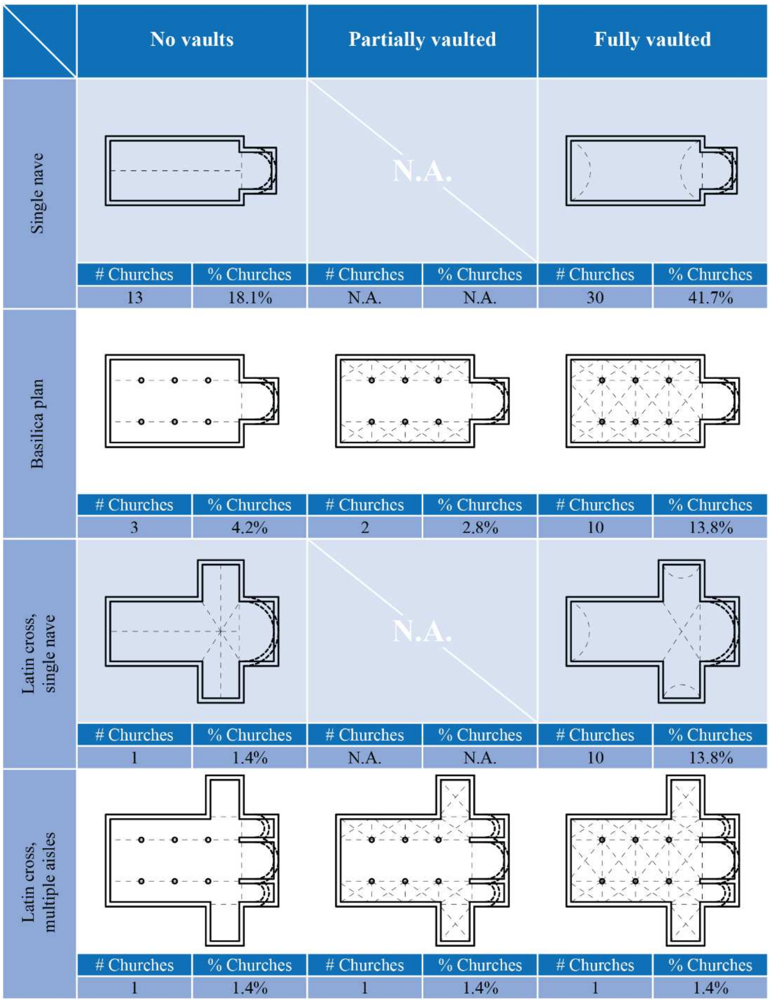


*Figure 3 – Typology, absolute number of churches, and relative number of churches surveyed categorized by floor plan and vault system.*

## 5. Seismic Risk Assessment

For purposes of this study, risk (R) was defined as the product of hazard (H), vulnerability (V), exposure (E), and consequences (C) [32, 33, 34, 23, 35]. With respect to earthquakes, these four different factors defined as "Risk Components" are described as follows:

- **Hazard (H)** refers to the probability that an earthquake causing a particular ground motion intensity will occur within a given reference period;
- **Vulnerability (V)** represents the expected performance and damage of a given structure caused by shaking of a certain intensity;
- **Exposure (E)** refers to the social and spiritual values, as well as to the loss of lives that may be related to building damage in each region;

- **Consequences (C)** addresses the value that may be lost in terms of reparation costs, social and urban capital, and, most importantly, the loss of the heritage value comprising the churches themselves and the pieces of art contained within them.

### *5.1. Risk Components: Definition and Quantification*

Given the primary goal of the research to develop a generalizable, rapid, and reliable seismic risk assessment methodology for churches, the definition of the risk components was based upon data that were both easily accessible and based on dependable proxies for desired attributes. The four factors of risk were each divided into several subcomponents (Table 1), which are defined in the following sections.

To prevent any outliers from disproportionately affecting the calculation of the indices, the data collected from the 72 surveyed churches were fit to lognormally distributed functions. Each data set was normalized from 0 to 1 using as the normalizing bounds the values of the 5$^{th}$ and 95$^{th}$ percentiles [36, 37, 38]. All the values exceeding the 95$^{th}$ percentile were assigned to an index value of 1.0. All the values lower than the 5$^{th}$ percentile were assigned to an index value equal to the ratio between the 5$^{th}$ and the 95$^{th}$ percentiles. Intermediate values were linearly interpolated between the two bounds.

| Risk Component | Risk Subcomponent | Notation |
|---|---|---|
| Hazard | Index of hazard for 90 years average return period | $i_{H,90}$ |
| | Index of hazard for 151 years average return period | $i_{H,151}$ |
| | Index of hazard for 1424 years average return period | $i_{H,1424}$ |
| | Index of hazard for 2475 years average return period | $i_{H,2475}$ |
| Vulnerability | Index of vulnerability in the best-case scenario | $i_{V,min}$ |
| | Index of vulnerability in the worst-case scenario | $i_{V,max}$ |
| Exposure | Index of average occupancy rate during the week | $i_{OR,AO}$ |
| | Index of maximum occupancy rate throughout the year | $i_{OR,MO}$ |
| | Index of community use during the regular weeks' masses (i.e., from Monday to Sunday) | $i_{CU,RW}$ |
| | Index of community use during the highest attended holy days' masses (i.e., Christmas or Easter) | $i_{CU,HD}$ |
| Consequences | Index of minimum equivalent economic value | $i_{EEV,min}$ |
| | Index of maximum equivalent economic value | $i_{EEV,max}$ |
| | Index of susceptible heritage | $i_{SH}$ |

*Table 1 – Risk subcomponents.*

### *5.2. Hazard*

The peak ground acceleration (PGA) at various average return periods was selected as the hazard metric for the proposed methodology for the following reasons:

- practitioner familiarity;
- commonly quantified for any location in multiple countries;
- independence from structural performance;
- its common application for seismic fragility of unreinforced masonry (e.g., [16, 17]); and
- use for territorial scale analysis in recent studies [39].

Several different hazard metrics have been used in other research such as the Modified Mercalli Intensity *MMI* [11], the Mercalli-Cancani-Sieberg Intensity *MCS* [4, 40], the current Italian reference according to the European Macroseismic Scale EMS-98 [41, 42] and the spectral acceleration $S_a$ [22]. While a very complete historical seismicity catalogue exists in Italy [43], recurrence laws of macroseismic intensities are not avaiable systematically for all locations and the selection of proper periods of vibration for churches is a topic still in need of research. Other hazard metrics have been successfully correlated with damage, such as the Arias intensity or the Saragoni factor [44], but again occurrence laws are not systematically available for the practitioners. Furthermore, recent studies has shown the peak ground velocity (PGV) to have stronger correlations with the damage prediction of URM buildings [45], although the same studies concluded that PGA also had good correlation with building damage. However, design basis PGVs have not yet been directly determined across the country for various average return periods. While the DPCM regarding the “Guidelines for the Assessment and the Reduction of the Seismic Risk of Cultural Hritage” [21] recommends accounting for three limit states and corresponding average return periods, no variable limit state analysis was performed in the current reported study. The PGAs of four average earthquake return periods, $T_R$, (90, 151, 1424, and 2475 years) were considered herein based on the Italian High Council of Public Work [46] and the Italian Codes for Construction [47] in order to establish a more comprehensive representation of aggregated earthquake hazard consistent with the larger number of return period events considered in international standards (e.g., [48, 49]). The values of PGAs for the surveyed church locations were normally distributed as shown in Figure 4.

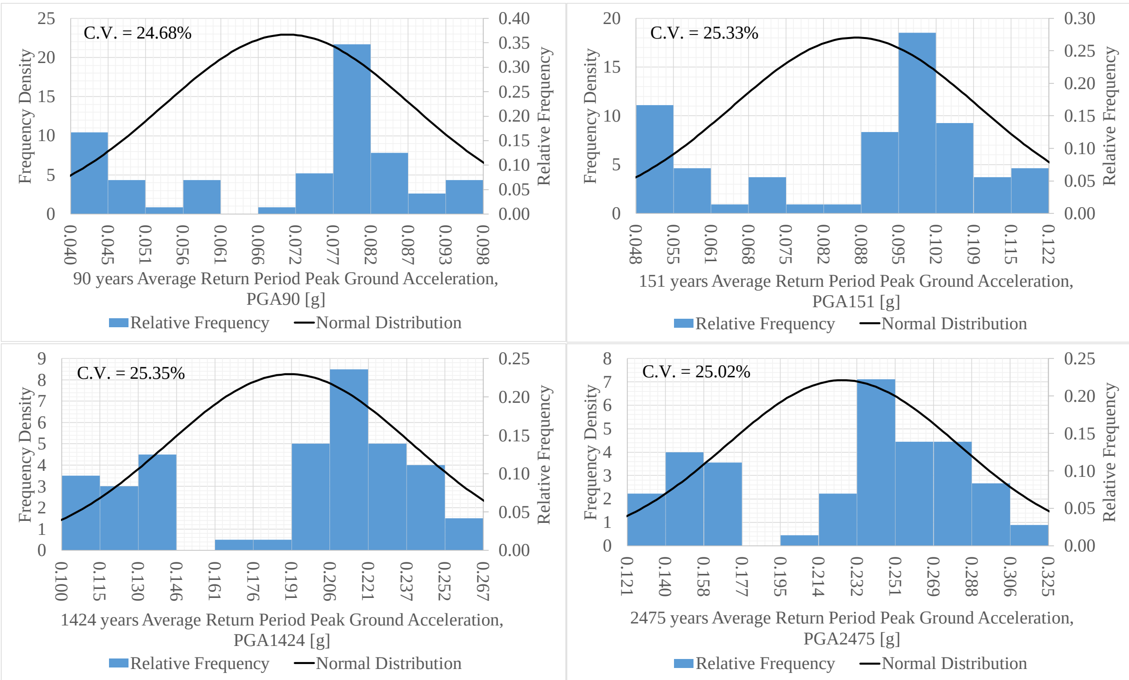


Figure 4 – Normal distribution and relative frequency of the PGA corresponding to $PGA_{90}$, $PGA_{151}$, $PGA_{1424}$, and $PGA_{2475}$.

The minimum subcomponent index value from each of the four distributions (i.e., return periods) shown in Figure 4 was determined as the 5th percentile of the 90 years average return period PGA, corresponding to $PGA_{5th}$ = 0.043g, while the maximum subcomponent index was set as the 95th percentile of the 2475 years average return period PGA, corresponding to $PGA_{95th}$ = 0.344g.

The indices of hazard $i_{H,i}$ were determined as described in section 5.1 and summarized in Appendix B.

### *5.3. Vulnerability*

Due to the slenderness of church walls compared to most other types of buildings, subdividing URM churches into units called “macro-blocks” is the practical method to assess churches and other complex URM buildings [1, 21, 50, 51, 52]. The macro-blocks considered in the current research are shown in Figure 5**Errore. L'origine riferimento non è stata trovata.**. Particularly vulnerable collapse mechanisms were identified through empirical observations during past earthquakes [1, 26, 28] and can be numerically predicted using virtual work principles. The DPCM [21], which is based on the work of Lagomarsino et al. [53], identified nine different macro-blocks (Figure 5) comprising 28 total collapse mechanisms (Appendix C - Figure C 1).

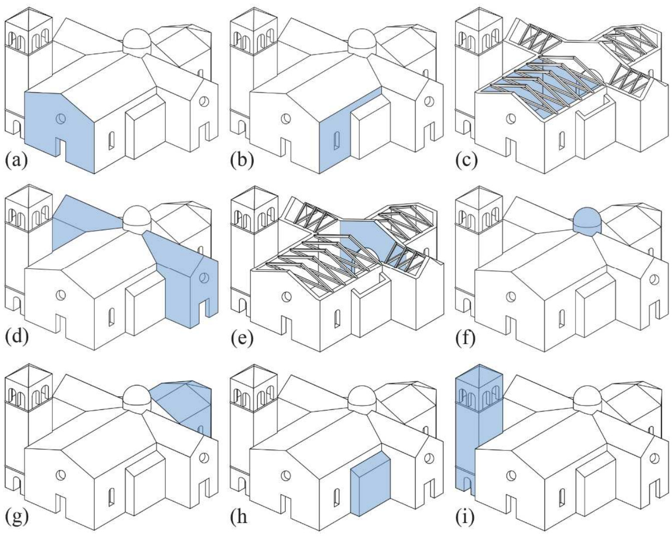


*Figure 5 – Macro-blocks considered: (a) Façade; (b) Lateral Walls; (c) Naves; (d) Transept; (e) Triumphal arch; (f) Dome; (g) Apse; (h) Chapels; (i) Bell Tower.*

According to the DPCM [21], the global seismic behavior of any church may be represented by a vulnerability index $i_V$ (ranging from 0 to 1) which accounts for the contribution of each macro-block collapse mechanism. Each macro-block collapse mechanism is affected by its geometric configuration, the material properties, the presence of structural elements, or previous retrofitting interventions. When the aforementioned parameters contribute toward increasing the vulnerability of the macro-block, they are classified as “vulnerability indicators”. When the aforementioned parameters contribute toward increase the robustness of the macro-block against collapse, they are classified as “robustness improvers”. An extensive list of the “vulnerability indicators”, and the “robustness improvers” is provided in Appendix C – Table C 1. Thus, the vulnerability index was determined using Equation 1:

$$i_{V,i} = \frac{1}{6}\frac{\sum_{k=1}^{28}\rho_{k,i}(v_{ki,i}-v_{kp,i})}{\sum_{k=1}^{28}\rho_{k,i}} + \frac{1}{2} \quad (1)$$

where: $i_{V,i}$ is the vulnerability index of the church ***i*** determined using the macro-blocks approach;

$\rho_{k,i}$ is the importance factor ($0 \leq \rho_{k,i} \leq 1$) of the *k*-th collapse mechanism on the global seismic behavior of the church *i*;

$v_{ki,i}$ is the score ($0 \leq v_{ki,i} \leq 3$) obtained by the evaluation of the vulnerability indicators;

$v_{kp,i}$ is the score ($0 \leq v_{kp,i} \leq 3$) obtained by the evaluation of the robustness improvers.

Values of $\rho_{k,i}$ for each macro-block collapse mechanism are listed in the DPCM [21]. The values of $\rho_{k,i}$ are dependent on the macro-block collapse mechanism and set as 1.0 for the most consequential (i.e., dangerous) mechanisms, with ranges between 0.5 and 1.0 in other cases. In the current research, values of $\rho_{k,i}$ proposed by the DPCM were used, and for the macro-block collapse mechanisms for which the 0.5 to 1.0 range of $\rho_{k,i}$ was offered, both the “best” (i.e., minimum vulnerability) and the “worst” (i.e., maximum vulnerability) possible scenarios were considered, by using accordingly values of 0.5 or 1.0. Thus, the indices of minimum and maximum vulnerability ($i_{V,min,i}$ and $i_{V,max,i}$) were determined using Equations 2 and 3, respectively.

$$i_{V,min,i} = \frac{1}{6}\frac{\sum_{k=1}^{28}\rho_{k,best,i}(v_{ki,min,i}-v_{kp,max,i})}{\sum_{k=1}^{28}\rho_{k,best,i}} + \frac{1}{2} \quad (2)$$

$$i_{V,max,i} = \frac{1}{6}\frac{\sum_{k=1}^{28}\rho_{k,worst,i}(v_{ki,max,i}-v_{kp,min,i})}{\sum_{k=1}^{28}\rho_{k,i}} + \frac{1}{2} \quad (3)$$

where: $i_{V,min,i}$ is the index of vulnerability of the church *i* for the best-case scenario;

$\rho_{k,best,i}$ is equal to $\rho_{k,max,i}$ if $v_{ki,min,i} \leq v_{kp,max,i}$, while $\rho_{k,best,i}$ is equal to $\rho_{k,min,i}$ if $v_{ki,min,i} \geq v_{kp,max,i}$;

$i_{V,max,i}$ is the index of vulnerability of the church *i* for the worst-case scenario;

$\rho_{k,worst,i}$ is equal to $\rho_{k,min,i}$ if $v_{ki,min,i} \leq v_{kp,max,i}$, while $\rho_{k,worst,i}$ is equal to $\rho_{k,max,i}$ if $v_{ki,min,i} \geq v_{kp,max,i}$.

A possible modification to the DPCM [21] procedure parameters was proposed by De Matteis et al. [54]. Wherein the vulnerability and robustness scores, $v_{ki,i}$ and $v_{kp,i}$, were determined using Equations 4 and 5.

$$v_{ki,i} = \frac{3}{5n_{ki}}\sum_{j=1}^{n_{ki}} I_{i,ki,j} \quad (4)$$

$$v_{kp,i} = \frac{3}{5n_{kp}}\sum_{j=1}^{n_{kp}} I_{e,kp,j} \quad (5)$$

where: $n_{ki}$ and $n_{kp}$ are, respectively, the number of vulnerability indicators, and the number of seismic robustness improvers associated with the *k*-th collapse mechanism, defined in Appendix C –Table C 1;

$I_{i,ki,j}$ is the influence score (varying from 1 to 5) of the *j*-th vulnerability indicators, defined in Appendix C –Table C 2;

$I_{e,kp,j}$ is the effectiveness score (varying from 1 to 5) of the *j*-th robustness improver, defined in Appendix C –Table C 3.

The criteria for assigning the influence and the effectiveness score ($I_{i,ki}$ and $I_{e,kp}$) were extensively detailed in Appendix C – Table C 2 and Table C 3. When $I_{i,ki}$ and $I_{e,kp}$ could not properly determined (e.g., judging the quality of the masonry was impossible when the observed macro-block was entirely plastered), both limit cases (i.e., a score of 1 or 5) were considered, resulting in the possible scores for the vulnerability indicators and the robustness improvers, $v_{ki,max,i}$, $v_{ki,min,i}$, $v_{kp,max,i}$, and $v_{kp,min,i}$. The authors emphasize that the criteria shown in Appendix C – Table C 2 and Table C 3, were developed for the purposes of a rapid and effective visual survey, based on the recurrent characteristics of the analyzed churches, the input of the DPCM [21], and consistently with the observations of previous researchers [1, 2, 51, 54]. The criteria retain a conventional component and further research to achieve more strict criteria is desirable.

The resulting indices of vulnerability $i_{V,i}$ were summarized in Appendix B

### *5.4. Exposure*

Two main subcomponents were considered to quantify the exposure of each church:

- The “Occupancy Rate” subcomponent accounts for the possible loss of lives due to the potential collapse of the church. Two occupancy rates were utilized in the risk assessment: 1) the average occupancy during the week; and 2) the maximum occupancy throughout the year;
- The “Community Use” subcomponent accounts for the utility of the church as a proportion of the size of the surrounding community. The loss of a church with a high community use may correspond with a significant functional service loss (i.e., interruption of the service of the Holy Mass for a large portion of the community). This parameter was used as a proxy for the spiritual value and the importance of the church as perceived by its community. Two scenarios were

investigated during the surveys: 1) the community use during the regular weeks' masses (i.e., from Monday to Sunday); and 2) the community use during the highest attended holy days' masses (i.e., Christmas or Easter).

### 5.4.1. *Indices of Occupancy Rate*

Since official attendance records at masses are not publicly available, the approximate numbers of churchgoers were determined by interviewing priests associated with each church. The priests were asked to report the average number of churchgoers per each day of the week, $p_{j,i}$, and the maximum attendance during the most crowded days of the year (i.e., Christmas and Easter), $p_{max,i}$. Equation 6 was used to determine the average occupancy rate in the church $i$ ($p_{av,i}$):

$$p_{av,i} = \frac{\sum_{j=1}^{7} p_{j,i}}{7} \quad (6)$$

where: $p_{j,i}$ is the number of churchgoers during the $j$-th day of the week in the church $i$.

The log-normal distribution of $p_{av,i}$ and $p_{max,i}$ were determined (Figure 6 and Figure 7) to proceed with the identification of the 5$^{th}$ and the 95$^{th}$ percentiles. For $p_{av,i}$, the minimum was determined as the 5$^{th}$ percentile, corresponding to $\ln(p_{av,5th}) = 0.72$ ($p_{av,5th} = 2.05$ people/day), while the maximum subcomponent index value was set as the 95$^{th}$, corresponding to $\ln(p_{av,95th}) = 4.91$ ($p_{av,95th} = 136.20$ people/day). For $p_{max,i}$, the minimum subcomponent index value was determined as the 5$^{th}$ percentile, corresponding to $\ln(p_{max,5th}) = 3.89$ ($p_{max,5th} = 49.03$ people), while the maximum was set as the 95$^{th}$ percentile, corresponding to $\ln(p_{max,95th}) = 6.44$ ($p_{max,95th} = 624.64$ people).

The indices of average and maximum occupancy rate ($i_{OR,AO,i}$ and $i_{OR,MO,i}$) were determined as described in section 5.1 and summarized in Appendix B.

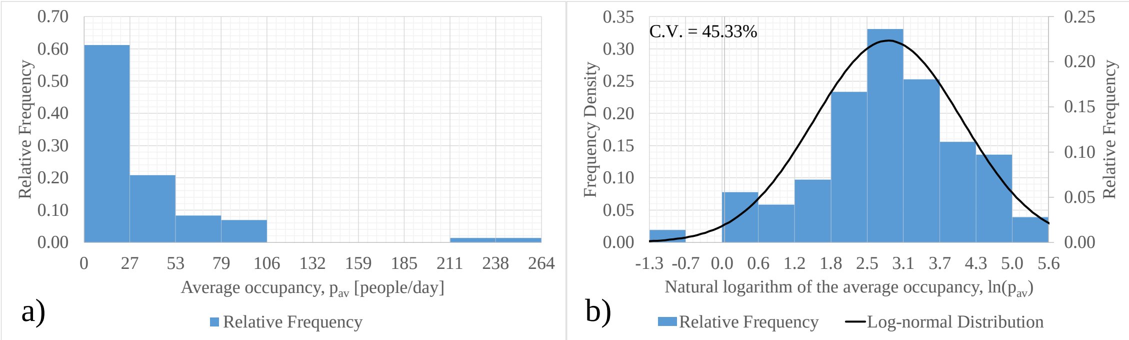


*Figure 6 – a) Relative frequency of $p_{av,i}$; b) Log-normal distribution and relative frequency of $\ln(p_{av,i})$.*

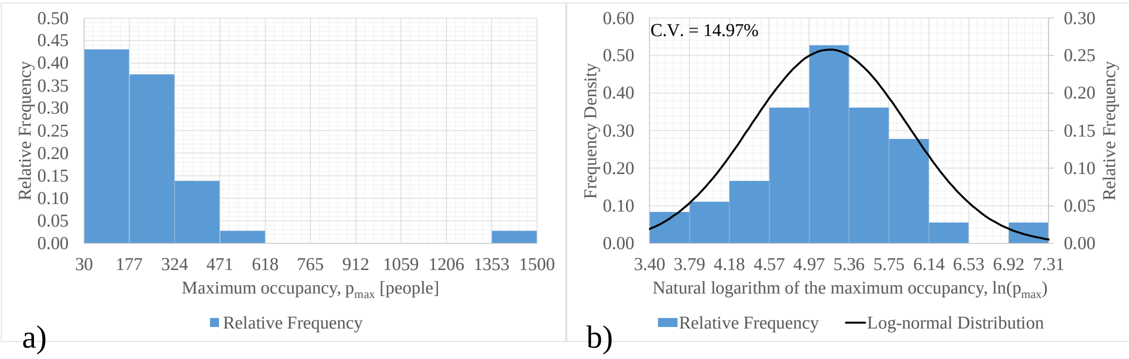


*Figure 7 – a) Relative frequency of $p_{max,i}$; b) Log-normal distribution and relative frequency of $\ln(p_{max,i})$.*

### *5.4.2. Indices of Community Use*

To determine the community use during the regular weeks' masses of the church *i*, $k_{av,i}$, and the community use during the holy days' masses of the church *i*, $k_{max,i}$, Equation 7 and Equation 8 were used, respectively:

$$k_{av,i} = \frac{p_{av,i}}{N_{set,i}} \quad (7)$$

$$k_{max,i} = \frac{p_{max,i}}{N_{set,i}} \quad (8)$$

where: $N_{set,i}$ is the number of residents of the city or settlement ("frazione") where the church ***i*** is located.

The log-normal distribution was determined (Figure 8 and Figure 9) to proceed with the measurement of the 5$^{th}$ and the 95$^{th}$ percentiles. For $k_{av,i}$, the minimum subcomponent index value was determined as the 5$^{th}$ percentile, corresponding to $\ln(k_{av,5th}) = -6.42$ ($k_{av,5th} = 0.0016$), while the maximum subcomponent index value was set as the 95th percentile, corresponding to $\ln(k_{av,95th})$ = -1.647 ($k_{av,95th}$ = 0.193). For $k_{max,i}$, the minimum subcomponent index value was determined as the 5th percentile, corresponding to $\ln(k_{max,5th})$ = -4.230 ($k_{max,5th}$ = 0.015), while the maximum subcomponent index value was set as the 95th, corresponding to $\ln(k_{max,95th})$ = 0.862 ($k_{max,95th}$ = 2.368).

In Figure 9, it might be noticed that $k_{max,i}$ may be larger than 1, which might be true for small settlements whose residents usually have an older average age. In fact, in this kind of villages the Christmas and Easter masses are regularly attended by the whole family, while, throughout the rest of the year, the younger members of the family live and attend masses in different cities.

The indices of the community use during the regular weeks' masses and the holy days' masses ($i_{CU,RW,i}$ and $i_{CU,HD,i}$) were determined as described in section 5.1 and summarized in Appendix B.

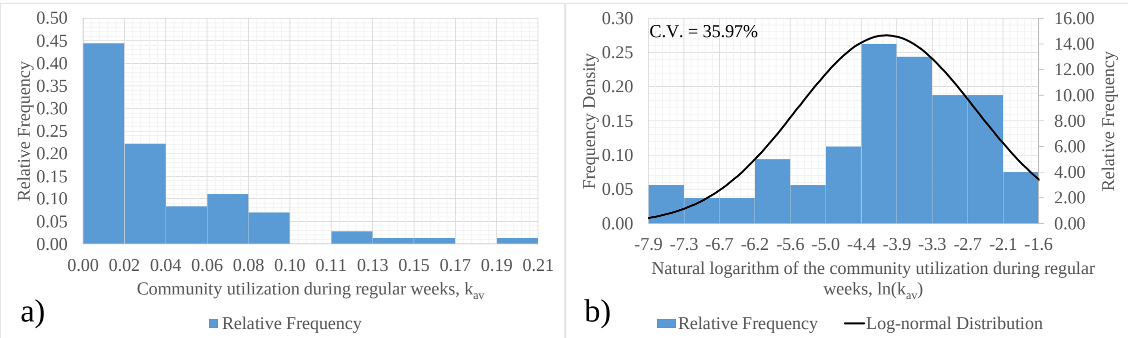


*Figure 8 – a) Relative frequency of $k_{av,i}$; b) Log-normal distribution and relative frequency of $\ln(k_{av,i})$.*

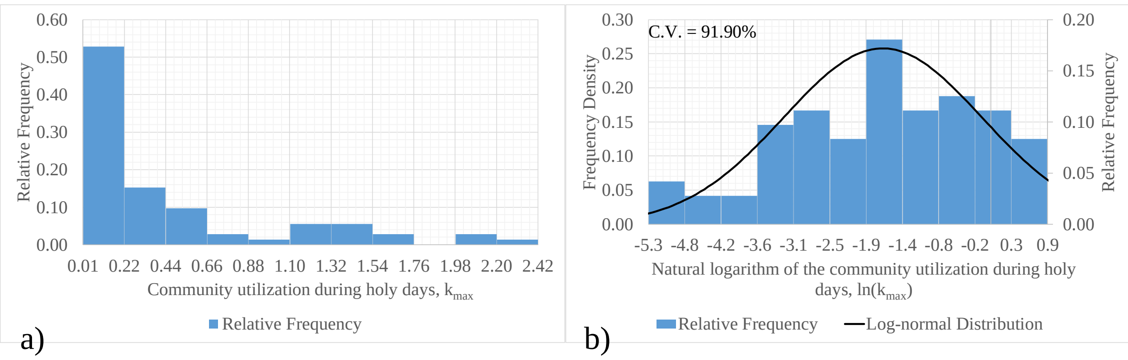


*Figure 9 – a) Relative frequency of $k_{max,i}$; b) Log-normal distribution and relative frequency of $\ln(k_{max,i})$.*

### *5.5. Consequences*

Two main aspects were considered to address the consequences component of risk:

- The "Equivalent Economic Value" (EEV) accounts for the possible cost of reconstruction of the church due to its hypothetical collapse; and
- The "Susceptible Heritage" subcomponent accounts for the presence of heritage art and architecture within the church (e.g., paintings, sculptures, architectural value).

#### *5.5.1. Indices of Equivalent Economic Value*

Historic religious, artistic, cultural, and architectural heritage elements contained in each church cannot and should not be estimated in a monetary way. To address the lack of functional service capacity offered to the communities because of a hypothetical destructive event leading to the irreparable collapse of the church, the equivalent economic value (EEV) as used in the current research was intended to be representative of the cost of reconstruction of a new building. Furthermore, the authors recognize their lack of expertise in determining the actual market value of complex buildings such as churches. While the authors encourage further research on the topic, the EEV should be interpreted as an initial attempt to quantify a fundamental aspect of any risk assessment (i.e., the economic consequences) in the current methodology.

Given the lack of data regarding the cost of construction of churches, the equivalent value was based on the value per square meter (€/m$^2$) of a residential three-story building having the same footprint as each church. The equivalency with a three-story building was chosen based on approximating the equivalent volume of a church. Also, the normalized value of the land, $i_{a,i}$, was subtracted from the EEV, assuming that the church would be reconstructed on the same site (neglecting a minority of cases in which the soil damage would force the a relocation). This approach was considered reasonable for three main reasons:

- The data regarding the value per square meter of residential buildings are easily accessible for each church location, thus enhancing the speed and the generalizability of the proposed methodology;
- Given the relative index scoring of the proposed methodology, the actual price of construction of each church is less relevant than the proportional construction cost between different churches. Furthermore, estimating the price of construction requires more detailed geometric information regarding the building (e.g., [55]) which would heavily reduce the efficiency of applying the proposed methodology; and
- The equivalent value of a new residential building construction represents the material cost, and the labor cost within the geographical region where the church is located and, thus, adequately represents the proportional comparison for the construction of a new church in different Italian geographic regions.

The minimum and the maximum value per square meter of the residential buildings ($C_{eq,min,i}$ and $C_{eq,max,i}$) were based on the data collected by the Italian Real Estate Market Observatory [56] and by the local Chambers of Commerce [57]. The value of the land, $i_{a,i}$, was determined as a percentage of the value of the church. Although the value of $i_{a,i}$ is highly variable, several researchers have recommended the use of values between 0.1 and 0.3 [58, 59, 60, 61]. For purposes of the current research, the economic impact of the land $i_{a,i}$ was assigned in accordance with the commercial value of the examined area as follows:

- $i_{a,i} = 0.30$ for the central business district of main cities and valuable areas;

- $i_{a,i} = 0.20$ for the central business district of minor cities;
- $i_{a,i} = 0.15$ for suburban areas;
- $i_{a,i} = 0.10$ for rural areas.

Thus, to determine the minimum and the maximum equivalent values of church *i* ($V_{EEV,min,i}$ and $V_{EEV,max,i}$), Equations 9 and 10 were used. Please, note that $V_{EEV,min,i}$ and $V_{EEV,max,i}$ were expressed in ₠ (Equivalent Currency) to highlight their status of relative equivalent values.

$$V_{EEV,min,i} = 3S_i C_{eq,min,i}(1 - i_{a,i}) \quad (9)$$

$$V_{EEV,max,i} = 3S_i C_{eq,max,i}(1 - i_{a,i}) \quad (10)$$

where: $S_i$ is the surface of the church *i*;

$C_{eq,min,i}$ is the minimum value per square meter of the church *i*;

$C_{eq,max,i}$ is the maximum value per square meter of the church *i*;

$i_{a,i}$ is the economic impact of the land on the total value of the church *i*;

Since the corresponding values of $V_{EEV,min,i}$ and $V_{EEV,max,i}$ resulted in a skew normal distribution, the log-normal distribution was determined (Figure 10 and Figure 11) to proceed with the measurement of the $5^{th}$ and the $95^{th}$ percentiles. The minimum subcomponent index value was determined as the $5^{th}$ percentile of $V_{EEV,min}$, corresponding to $\ln(V_{EEV,5th}) = 12.24$ ($V_{EEV,5th}$ = 207,225 ₠), while the maximum subcomponent index value was set as the $95^{th}$ percentile of $V_{EEV,max}$, corresponding to $\ln(V_{EEV,95th}) = 14.79$ ($V_{EEV,5th}$ = 2,656,528 ₠).

The indices of minimum and maximum equivalent economic value ($i_{EEV,min,i}$ and $i_{EEV,max,i}$) were determined as described in section 5.1 and summarized in Appendix B.

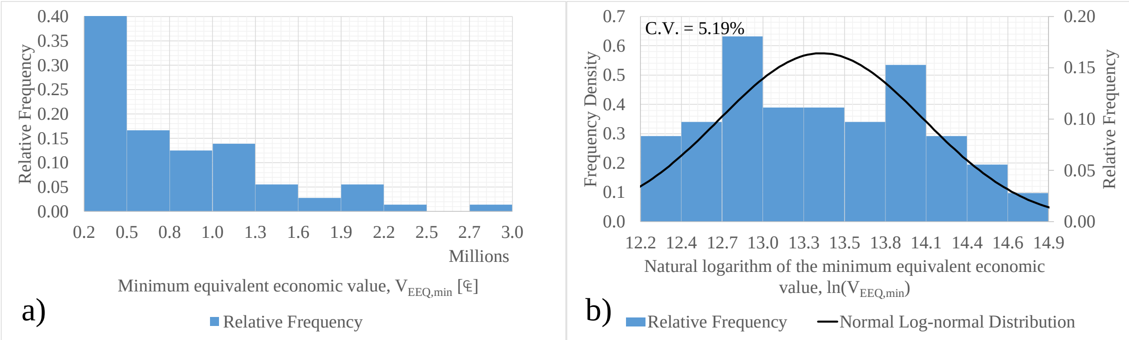


*Figure 10 – a) Relative frequency of $V_{EEQ,min,i}$; b) Log-normal distribution and relative frequency of $\ln(V_{EEQ,min,i})$.*

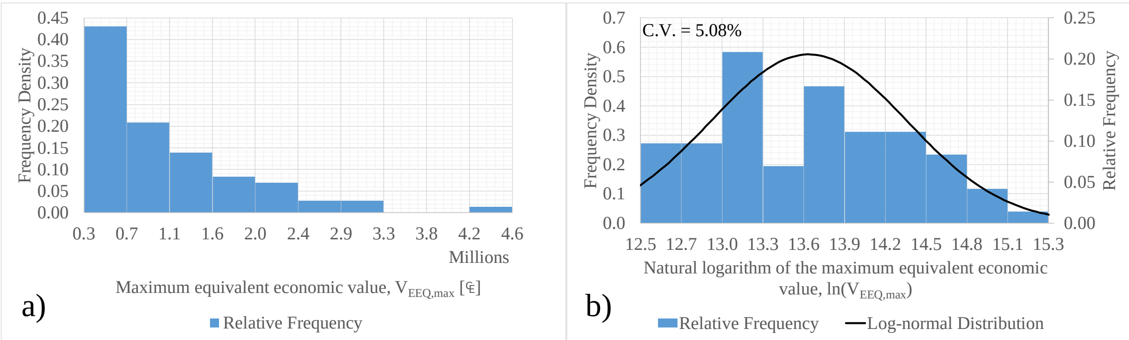


*Figure 11 – a) Relative frequency of $V_{EEQ,max,i}$; b) Log-normal distribution and relative frequency of $\ln(V_{EEQ,max,i})$.*

### *5.5.2. Index of Susceptible Heritage*

The presence of heritage art and architectural features within the assessed churches was based on a proposed scoring system (Figure 12). In these terms, the discriminating feature that helped in comparing the churches was their ornamental systems which characterized and distinguished the Italian Romanesque and Gothic architecture from the rest of the western Europe [62]. The creation of figural art (e.g., sculptures, paintings, and mosaics) was not an aesthetic formality, especially during the Middle Ages, but rather a means to transmit knowledge about the sacred writings to the churchgoers [63]. Thus, the presence, the quality, and the quantity of the decorative features were considered and compared following what was perceived as their most important attributes:

- The façade is the main face of a church designed to guide the churchgoers toward their spiritual journey [64]. The dual role of welcoming churchgoers and making the church's façade distinct was usually achieved by using different types of ornamentations (e.g., sculptures, painted glasses, architectural ornament, and others) [63]. The comparative quantities of façade ornamentation were surveyed as part of the current study;

- Vaulted ceilings required a significant amount of labor to be constructed [65]. Therefore, the presence of vaulted ceiling (most often in the naves and apses) represents an added value for the church, and especially so in the case of vaults decorated with frescoes;
- The figurative apparatus on the internal walls was considered the natural extension of the spiritual journey initiated by the façade, representing a crucial component in leading the devotees through the mass [63];
- Given the lack of information for comparing the values of paintings, their quantity was recorded; and
- One-third of the total subcomponent index score was left to the surveyor's discretion in case of recognizable pieces of art composed by famous masters (e.g., the rare tridimensional painting of the holy Mary with the Child in the church of San Giovanni Evangelista in Vico Equense, or the Michelangelo's lion sculpture in the church of Santa Maria Maddalena in Capranica Prenestina). Each case was evaluated and judged following in-depth research on the artefact. Although not explicitly required for the assessment, the authors suggest making use of the "Guida Rossa" [66], a colletion of catalogues containing a description and an importance rating of a large variety of pieces of art housed in the various regions across Italy. Where available, the archives of the dioceses were used as a guide for identifying artworks of cultural and historical importance.

| Qualitative Question | Qualitative Parameter | Parameter Score | Max Score |
|---|---|---|---|
| Are there ornaments on the façade? | No | +0 points | 10 points |
| | Architectural ornamentation | +2 points | |
| | Sculptured ornamentation | +3 points | |
| | Painted ornamentation | +3 points | |
| | Other | +2 points | |
| Is the vault painted? | No vault | +0 points | 5 points |
| | Vault without frescoes | +2 point | |
| | Vault with frescoes | +5 points | |
| Are there ornaments on the internal walls or chapels? | No ornamentation on the wall and no chapels | +0 points | 10 points |
| | No ornamentation on the walls nor on the chapels | +1 points | |
| | Architectural ornamentation | +2 points | |
| | Sculptured ornamentation | +3 points | |
| | Walls/chapels with frescoes | +3 points | |
| | Other | +2 points | |
| Are there paintings in the church? | No | +0 points | 5 points |
| | ≤ 5 | +1 point | |
| | ≤ 10 | +2 points | |
| | ≤ 15 | +3 points | |
| | ≤ 20 | +4 points | |
| | > 20 | +5 points | |
| Is there any recognizable piece of art (e.g., paintings or sculptures made by famous artists)? | Number of recognizable pieces of art | Based on educated judgment (The "Guida Rossa" [64] and the diocese's archives might be used to help in the judgment) | 15 points |
| **MAXIMUM TOTAL SCORE** | | | **45 points** |

*Figure 12 – Criteria for the scoring system of the susceptible heritage.*

Since the minimum and the maximum of values the scoring method for the index of susceptible heritage were well defined (respectively 0 and 45 points), no statistical analysis to determine the 5$^{th}$ and the 95$^{th}$ percentiles was required. Therefore, the index of susceptible heritage $i_{SH,i}$ was determined using Equation 11.

$$i_{SH,i} = \frac{Score_i}{45} \quad (11)$$

where: $Score_i$ is the total score reached by the church *i* with respect of Figure 12.

The resulting indices of susceptible heritage $i_{SH,i}$ were summarized in Appendix B.

### *5.6. Fuzzy Set Theory: Definition and Application Methodology*

The FST is a statistical procedure developed for combining variables with a large component of uncertainty [24, 67, 68]. In contrast to the classic set theory, which postulates that a variable $x$ can be part of a set $A$ or not, the FST provides a membership ratio $\mu_i$ (ranging from 0 to 1) to one or more sets $A_i$, addressing the variability of $x$ by leaving room for the inherent uncertainties and the complexity of the assessing procedure. Thus, the sets used for compressing the inputs $x_i$ (i.e., the risk component indices) are applied in order to consider two variables simultaneously in an iterative procedure resulting in one single output (i.e., the seismic risk rating) [67]. A schematic representation of the iterative procedure is shown in Figure 13.

Differently from other assessment techniques, such as the models for macroseismic vulnerability and damage assessment based on the fragility and capacity curves [41, 69, 70], the FST allows to account for more than two variable at the same time, including the four components of risk instead of limiting the assessment to the hazard and the vulnerability.

The aggregation procedure comprises four steps. An exhaustive explanation of the FST and a worked example for a case study church implementing all steps is included in Appendix D and E.

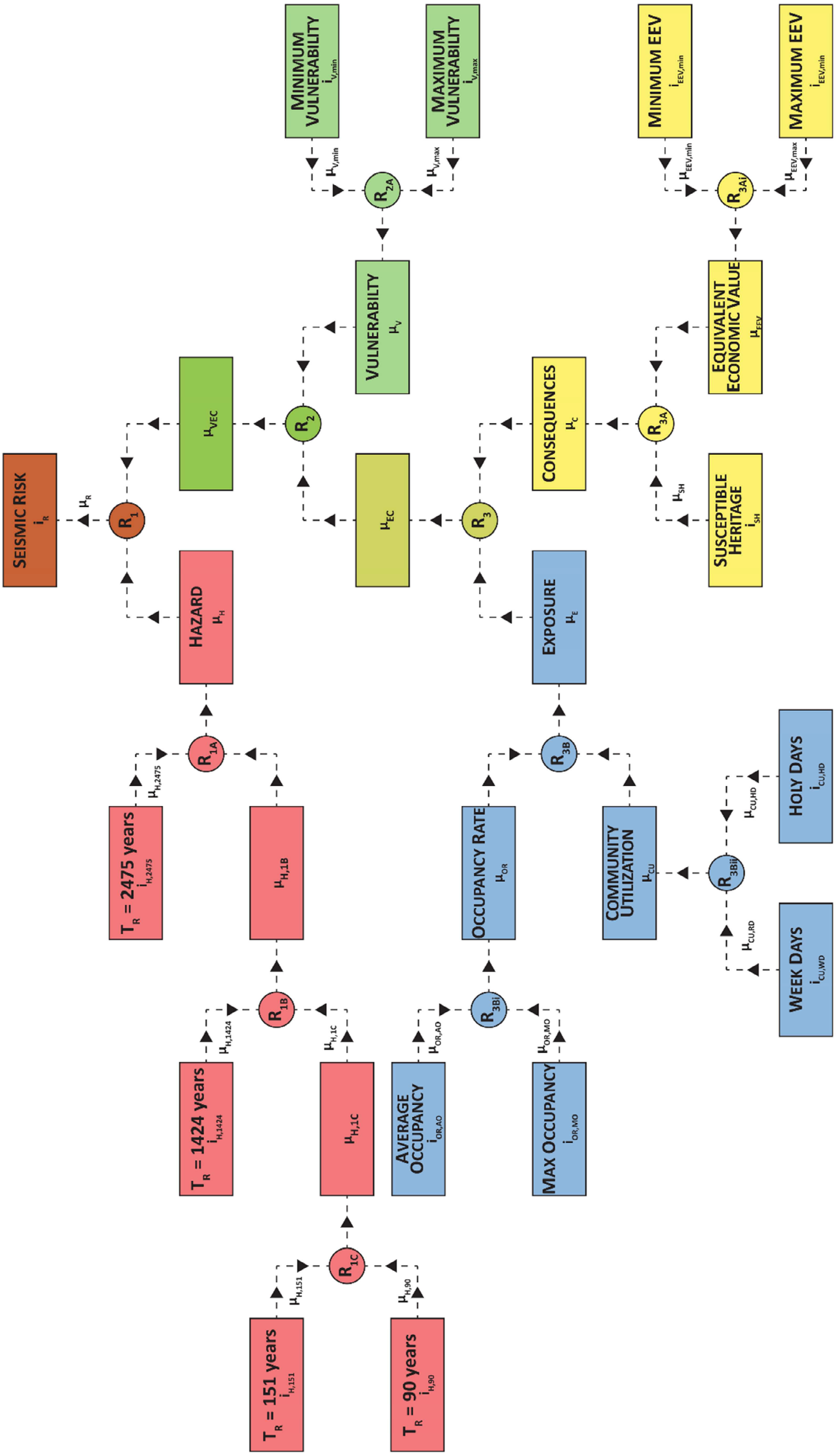


*Figure 13 – The FST procedure for determining the seismic risk rating in the current study.*

### *5.7. FST Results and Multilinear Regression of Ratings*

The resulting indices of seismic risk, $i_{R,i}$, are shown in Figure 14**Errore. L'origine riferimento non è stata trovata.**. Veneto was determined to be the region with the largest average risk rating across its surveyed portfolio of churches. Also, the average risk rating for churches in Lazio was comparatively high, mostly because of index ratings of hazard and susceptible heritage of the churches within this region. The lowest regional average risk rating was determined to be in Toscana. The lowest risk rating for a single church was determined to occur in Trentino – Alto Adige due to the comparatively low seismicity of this region (Figure 1). Note that the church determined to have the highest comparative risk rating in the Lazio region was independently identified by the diocese of Anagni-Alatri to be prioritized for strengthening intervention within their portfolio.

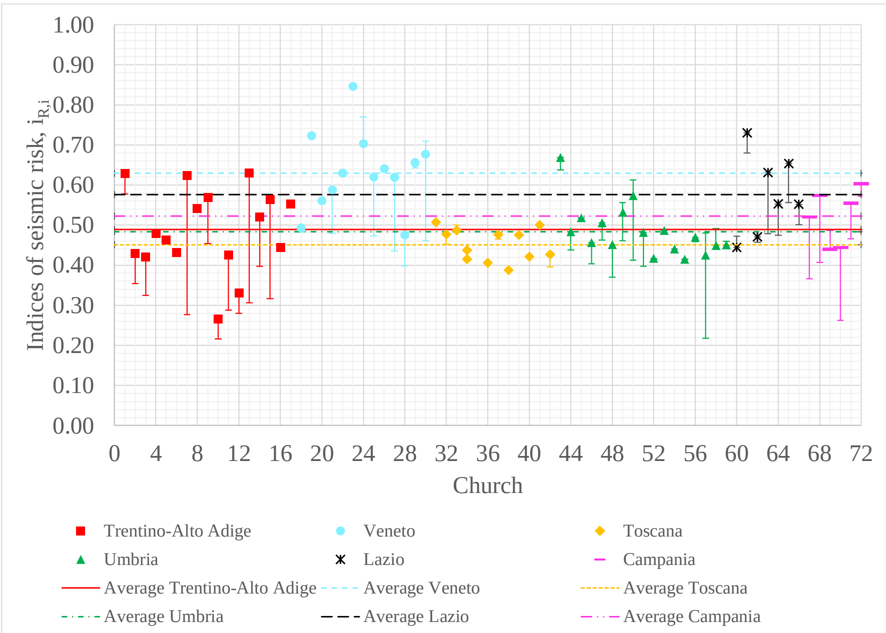


*Figure 14 – Seismic risk ratings $i_{R,i}$ and average risk sorted by region.*

Given the various uncertainties inherent to the risk subcomponents, the variability of the risk ratings, $i_{R,i}$, was also charted in Figure 14. Greater uncertainty in parameters (e.g., the quality of the masonry of a plastered wall), corresponds to wider ranges between the lower and the upper risk rating limit. However, the implementation of the risk aggregation procedure resulted in the final risk ratings, $i_{R,i}$, being generally closer to the upper limit. Therefore, the methodology accounted for the unknowns (depending on the conditions of each inspected church) throughout using a comparatively conservative approach, in accordance with common engineering practice. Please note that, although not evident in Figure 14, both lower and upper whiskers are present for each church, however, for some churches it was possible to collect a more information lowering the amount of uncertainties (therefore the extent of the whiskers) to the minimum.

Acknowledging that the FST procedure, as shown in Appendix D, can be prohibitively time-consuming for use by general practitioners who wish to carry the proposed preliminary portfolio risk analyses of similar churches in Italy, a multilinear regression was applied to the intermediate and the final outcomes of the FST analysis determined in the current study (Figure 14) to provide a direct correlation between the risk components and the final seismic risk ratings (see Equations 12 – 16). The determination coefficients, $R^2$, and the standard deviations of the regression, *S*, are listed in Table 2.

$$i_{H,i} = -4.822 i_{H,90,i} + 8.778 i_{H,151,i} - 7.256 i_{H,1424,i} + 5.020 i_{H,2475,i} \leq 1 \qquad (12)$$

$$i_{V,i} = 0.103 i_{V,min,i} + 0.892 i_{V,max,i} \leq 1 \qquad (13)$$

$$i_{E,i} = 0.029 i_{OR,AO,i} + 0.522 i_{OR,MO,i} + 0.302 i_{CU,RD,i} + 0.154 i_{CU,HD,i} \leq 1 \qquad (14)$$

$$i_{C,i} = -0.111 i_{EEV,min,i} + 0.593 i_{EEV,max,i} + 0.511 i_{SH,i} \leq 1 \qquad (15)$$

$$i_{R,i} = 0.297 i_{H,i} + 0.474 i_{V,i} + 0.155_{E,i} + 0.104 i_{C,i} \leq 1 \qquad (16)$$

| Equation | Ratings | $R^2$ | Standard deviation, S |
|---|---|---|---|
| 12 | Hazard, $\mathbf{i_{H,i}}$ | 0.957 | 0.091 |

| Equation | Ratings | $R^2$ | Standard deviation, S |
|---|---|---|---|
| 13 | Vulnerability, $\mathbf{i}_{V,i}$ | 0.981 | 0.038 |
| 14 | Exposure, $\mathbf{i}_{E,i}$ | 0.939 | 0.069 |
| 15 | Consequences, $\mathbf{i}_{C,i}$ | 0.967 | 0.064 |
| 16 | Seismic risk, $\mathbf{i}_{R,i}$ | 0.973 | 0.059 |

*Table 2 – Correlation factors,* $R^2$*, and standard deviation of the regression,* S.

Given that the correlation factor $R^2$ is by itself not sufficient to represent the quality of the fitting, the authors suggest referring to the standard deviation of the regression, $S$, to quantify the discrepancy between the proposed multilinear equations and the FST analysis. A detailed worked example comparing the results of the FST analysis and the ones of the proposed Equations 12 – 16 is shown in Appendix E.

## 6. Applications and Limitations

The model presented in this study was developed with reference to a specific typology, isolated medieval URM churches, but the methodology framework is general and could be adapted to different scenarios, provided that hazard, vulnerability, exposure and consequences are properly described and FST is applied.

The developed model was based on a sample composed of URM Italian medieval churches with an average footprint surface area of 410 m$^2$ and maximum footprint surface of 1340 m$^2$, located in settlements with an average of 4,000 residents and a maximum of 46,000 residents. If the proposed methodology were to be applied to larger URM non-medieval churches located in larger cities (e.g., cathedrals of main cities such as Rome or Milan), the authors recommend re-calibrating the limits given by the 5$^{th}$ and the 95$^{th}$ percentiles of the following indices:

- Index of average and maximum occupancy ratio, $i_{OR,AO}$ and $i_{OR,MO}$;
- Index of community use during the regular weeks' masses and holy days' masses, $i_{CU,RW}$ and $i_{CU,HD}$; and

- Index of minimum and maximum equivalent economic value, $i_{EEV,min}$ and $i_{EEV,max}$.

Note that the normal (or log-normal) distribution does not appropriately fit the collected data in some cases (Figure 4, Figure 6, Figure 7, Figure 8, Figure 9, Figure 10, and Figure 11) due to the sample size and the non-uniform geographic distribution of the surveyed churches across the country. A possible solution would be to limit the application of the procedure to a regional scale and re-calibrate the limits given by the 5$^{th}$ and the 95$^{th}$ percentiles of the aforementioned indices. The authors recommend further studies on a wider and more evenly distributed nationwide study sample before applying the procedure at a national scale.

Eventually, the methodology might also be applied in non-seismic hazard scenarios by defining an appropriate index (from 0 to 1) to account for the considered hazard (e.g., flooding, or hurricanes). Lastly, the proposed methodology may be applied for determining the risk rating associated with non-URM churches (i.e., churches constructed with other materials), but a different procedure for quantifying vulnerability should be applied.

A flow-chart that summarizes the entire application of the methodology and the actions required to acquire the data necessary to define each risk subcomponents is provided in Figure 15.

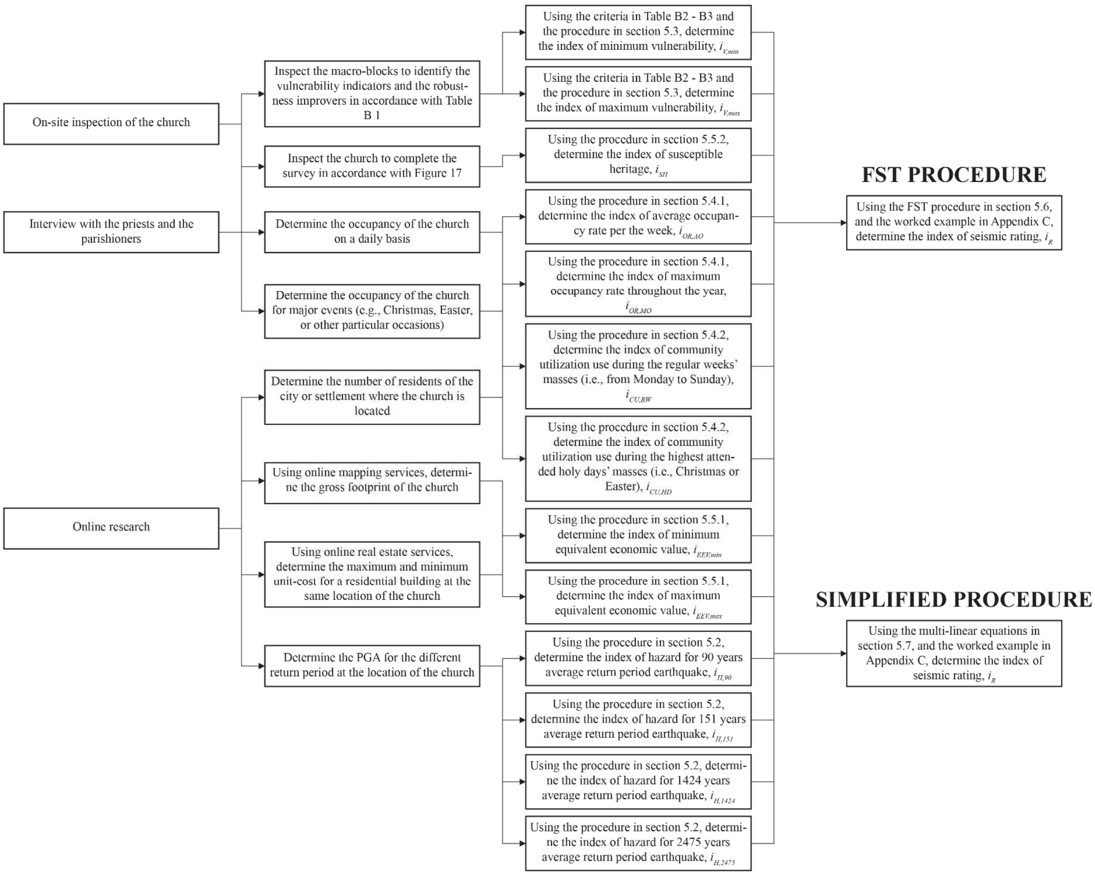


*Figure 15 – Flow-chart of the proposed risk assessment methodology.*

## 7. Conclusions and Related Research

In this paper, a holistic and generalizable seismic risk assessment methodology was established based on surveys of 72 URM Italian medieval churches. Indices to represent the different components of risk (i.e., hazard, vulnerability, exposure, and consequences) were developed and assessed with statistical bases. The indices were then processed through the "Fuzzy Set Theory" (FST) to account for statistical variations (including unknowns) and to produce a final comparative rating of seismic risk for each church. Lastly, a set of ready-to-use multilinear equations was developed to facilitate rapid assessment for similar scenarios conducted by others.

Using the proposed methodology, one single person could survey several churches per day to obtain the necessary information for the assessment, saving time and money for portfolio managers. Given the limited funding at the disposal of the selected communities, the developed seismic risk ratings are expected to offer a provisional basis to assist the decision-making process resulting in a cost-efficient management of the dioceses' property portfolio and funding allocations. The seismic risk ratings shown in Figure 14 will be provided to the portfolio managers of the respective dioceses and used to prioritize the churches for further detailed analysis and strengthening interventions of the identified vulnerabilities.

In addition to the final seismic risk rating, the indices of risk subcomponents shown in Appendix B and the indices of risk components obtainable using Equations 12 through 16 may have applicable value as well pertaining to which type of intervention may be most adequate. A non-exhaustive list of generic intervention options is offered below:

- **High risk subcomponent indices of hazard and/or vulnerability**: More sophisticated structural analysis and structural strengthening may be appropriate to enhance the capacity of the most critical macro-blocks of the church. The current literature offers a large variety of viable solutions depending on the conditions and the vulnerability of each church (e.g., [26, 71, 72]);
- **High risk subcomponent index of exposure**: A viable and relatively inexpensive policy to reduce the exposure in a church – mainly in regard to life safety – may be considered (e.g., to offer masses during holy days to reduce the number of churchgoers at any single mass); and
- **High risk subcomponent index of consequences**: The stipulation of insurance for construction damage may be a viable policy to reduce the amount of monetary losses where the combination of hazard and vulnerability is unfavorable. Furthermore, for irreplaceable pieces of art that enrich the churches' artistic and

heritage value, some consideration regarding the substitution of copies may be evaluated, while the originals may be stored in less vulnerable local venues.

The authors acknowledge that the amount of information required to apply the proposed methodology may deter some potential users; however, all the informational parameters can be completed using open-access data, rapid visual surveys of the churches, and interviews of the parish priests, making the indices themselves reproducible in an efficient fashion for many churches. The authors also acknowledge the parametric sensitivity of the seismic risk ratings for some churches (Figure 14), largely due to uncertainties in some of the church characteristics. Nonetheless, the proposed methodology is an initial holistic risk assessment at territorial scale. The authors' goal was to improve upon the value provided by the traditional LV1 ("Level One") analysis per DPCM [21] (which produces high variability in its results as well). In a world in which heritage portfolios age and expand constantly, with needs that generally exceed available resource, asset managers and engineers must prioritize the allocation of limited resources based on holistic portfolio risk profiles in order to determine which assets warrant more targeted assessments and interventions.

Material analysis based on non-destructive testing (NDT) techniques was developed to achieve a better understanding of the mechanical properties of URM (e.g., compressive strength) [73]. Furthermore, a photogrammetric three-dimensional model of a specific case study church was developed to achieve more precise geometric measures [74]. The mechanical and geometric properties were further used to develop a complete structural building information model (BIM) of this case study church, and to achieve an exhaustive structural analysis to compare the results of the detailed analysis with the results of the current provisional assessment.

**Acknowledgments**

This research was primarily funded by a Global Gateways Faculty Research Award at the University of Notre Dame (grant FY18RGG03). Undergraduate students at the University of Notre Dame who assisted with the surveys include Elizabeth DePaola, Emily Brady, Lily Polster, Marie Bond, and Patricia Dirlam. These students were supported by research scholarship funding from various programs, institutes, and centers at the University of Notre Dame, including the Fitzgerald Institute for Real Estate, the Grand Challenges Scholars Program, the Women in Engineering Program, and the Flatley Center for Undergraduate Scholarly Engagement.

The authors are thankful for the assistance of the cultural heritage offices of the involved dioceses, as well as the assistance of Dr. Federica Romiti (diocese of Anagni – Alatri), the Bishop Stefano Manetti and the Surveyor Marco Cortellessa (diocese of Montepulciano – Chiusi – Pienza), Don Francesco Valentini and the Dr. Giovanna Bandinu (diocese of Orvieto – Todi), the Arch. Agapito Fornari (diocese of Palestrina), Don Riccardo Pascolini (diocese of Perugia – Città della Pieve), Don Fabio Sottoriva (diocese of Vicenza), the Dr. Monia Sartori (archdiocese of Trento), the Arch. Graziana Santamaria, and the Surveyor Marco Cherubini. The first author would like to thank his parents Valter Pirchio and Lorena Trentini for their assistance with logistics, as well as an undergraduate student at the University of Trento, Chiara Meloni. The following priests are thanked for granting access to their churches and for assisting during the data collection:

- Diocese of Anagni – Alatri: Deacon Massimiliano Floridi, Don Alessandro De Sanctis, Don Antonio Castagnacci, Don Pierino Giacomi, Don Roberto Martufi, Don Virginio De Rocchis, and the parishes' collaborators.

- Diocese of Montepulciano – Chiusi – Pienza: Don Andrea Malacarne, Don Antonio Nutarelli, Don Azelio Mariani, Don Carlo Sensani, Don Elia Sartori, Don Francesco Monachini, Don Kishor Uppalapati, Don Manlio Sodi, Don Sergio Graziani, Don Silvano Nardi, Don Stefano Cinelli, and the parishes' collaborators.
- Diocese of Nocera Inferiore – Sarno: Friar Damiano Antonino, Friar Felice Petrone, Friar Michele Alfano, Friar Raffaele Panopio, Friar Renato Sapere, and the parishes' collaborators.
- Diocese of Orvieto – Todi: Don Claudio Calzoli, Don Jeremiah Joseph Kelly, Don Marcello Sargeni, Don Marco Gasparri, Don Piero Grassi, and Don Zeffiro Tordi.
- Diocese of Palestrina: Monsignor Andrea Leonardo (Diocese of Rome), Don Davide Maria Martinelli, and the parishes' collaborators.
- Diocese of Perugia – Città della Pieve: Don Augusto Martelli, Don Fabio Quaresima, Don Gianni Pollini, Don Giuseppe Piccioni, Don Marco Merlini, Don Matteo Rubechini, Don Vincenzo Esposito, and the parishes' collaborators.
- Diocese of Sorrento – Castellammare di Stabia: Don Antonino Lazzazzara, Don Beniamino Di Martino, Don Ciro Esposito, Don Maurizio Esposito, and the parishes' collaborators.
- Diocese of Trento: Don Ferdinando Murari, Don Maurizio Toldo, and the parishes' collaborators.
- Diocese of Vicenza: Don Adriano Preto Martini, Don Fabio Ogliani, Don Francesco Strazzari, Don Giacomo Viali, Don Giovanni Campagnolo, Don Giovanni Imbonati, Don Giovanni Sandonà, Don Giuseppe Mattiello, Don Luigi Spadetto, Don Paolo Zampiva, and the parishes' collaborators.

## References


[1] F. Doglioni, A. Moretti and V. Petrini, Le chiese e il terremoto. Dalla vulnerabilità constatata nel terremoto del Friuli al miglioramento antisismico nel restauro. Verso una politica di prevenzione., Trieste: Edizioni Lint, 1994.

[2] S. Lagomarsino, "Damage assessment of churches after l'Aquila earthquake (2009)," *Bulletin of Earthquake Engineering,* vol. 10, no. 1, pp. 73-92, 2012.

[3] M. A. V. Parisi, C. Tardini and E. Maritato, "Seismic behaviour and vulnerability of church roof structures," *Structural Analysis of Historical Constructions,* pp. 1582-1589, 2016.

[4] S. Lagomarsino and S. Podestà, "Seismic vulnerability of ancient churches: II. Statistical analysis of surveyed data and methods for risk analysis.," *Earthquake Spectra,* vol. 20, no. 2, pp. 395-412, May 2004.

[5] M. Valente and G. Milani, "Damage survey, simplified assessment, and advanced seismic analyses of two masonry churches after the 2012 Emilia earthquake," *International Journal of Architectural Heritage,* vol. 13, no. 6, pp. 901-924, 2019.

[6] A. Formisano, G. Vaiano, F. Fabbroccino and G. Milani, "Seismic vulnerability of Italian masonry churches: The case of the Nativity of Blessed Virgin Mary in Stellata of Bondeno," *Journal of Building Engineering,* vol. 20, pp. 179-200, 2018.

[7] S. Lagomarsino, A. Brencich, F. Bussolino, A. Moretti, L. C. Pagnini and S. Podestà, "Una nuova metodologia per il rilievo del danno alle chiese: prime considerazioni sui meccanismi attivati dal sisma," *Ingegneria sismica,* vol. 3, pp. 70-82, 1997.

[8] F. da Porto, B. Silva, C. Costa and C. Modena, "Macro-scale analysis of damage to churches after earthquake in Abruzzo (Italy) on April 6, 2009," *Journal of Earthquake Engineerin,* vol. 16, no. 6, pp. 739-758, 2012.

[9] L. Sorrentino, L. Liberatore, L. D. Decanini and D. Liberatore, "The performance of churches in the 2012 Emilia earthquakes," *Bulletin of Earthquake Engineering,* vol. 12, no. 5, pp. 2299-2331, 2014.

[10] G. De Matteis, G. Brando, V. Corlito, E. Criber and M. Guadagnuolo, "Seismic vulnerability assessment of churches at regional scale after the 2009 L'Aquila earthquake," *International Journal of Masonry Research and Innovation,* vol. 4, no. 1-2, p. 174–196, 2019.

[11] A. Penna, C. Calderini, L. Sorrentino, C. F. Carocci, E. Cescatti, R. Sisti, A. Borri, C. Modena and A. Prota, "Damage to churches in the 2016 central Italy earthquakes," *Bulletin of Earthquake Engineering,* vol. 17, no. 10, pp. 1-28, 2019.

[12] N. Chieffo, F. Clementi, A. Formisano and S. Lenci, "Comparative fragility methods for seismic assessment of masonry buildings located in Muccia (Italy)," *Journal of Building Engineering,* vol. 25, p. 100813, 2019.

[13] S. R. Abeling, S. Vallis, T. Goded, S. Giovinazzi and J. M. Ingham, "Seismic Risk Assessment of New Zealand URM Church," in *10th Australian Masonry Conference*, Sydney, 2018.

[14] A. Marotta, L. Sorrentino, Liberatore D. and J. M. Ingham, "Seismic risk assessment of New Zealand unreinforced masonry churches using statistical procedures," *International Journal of Architectural Heritage,* vol. 12, no. 3, pp. 448-464, 2018.

[15] L. Hofer, P. Zampieri, M. A. Zanini, F. Faleschini and C. Pellegrino, "Seismic damage survey and empirical fragility curves for churches after the August 24, 2016 Central Italy earthquake," *Soil Dynamics and Earthquake Engineering,* vol. 111, pp. 98-109, 2018.

[16] C. Del Gaudio, G. De Martino, M. Di Ludovico, G. Manfredi, A. Prota, P. Ricci and G. M. Verderame, "Empirical Fragility Curves for Masonry Buildings after the 2009 L'Aquila, Italy, Earthquake," *Bulletin of Earthquake Engineering,* vol. 17, no. 11, pp. 6301-6330, 2019.

[17] A. Rosti, M. Rota and A. Penna, "Empirical Fragility Curves for Italian URM Buildings," *Bulletin of Earthquake Engineering.,* 2020.

[18] A. Marotta, D. Liberatore and L. Sorrentino, "Development of parametric fragility curves for historical churches struck by seismic action," *Bulletin of Earthquake Engineering,* 2021 (in review).

[19] *Disposizioni concernenti la concessione di contributi finanziari della CEI per i beni culturali ecclesiastici e l'edilizia di culto e il relativo Regolamento attuativo,* 2018.

[20] P. C. N. (PCN), "Classificazione sismica," 6 June 2020. [Online]. Available: http://www.protezionecivile.gov.it/attivita-rischi/rischio-sismico/attivita/classificazione-sismica. [Accessed 15 October 2020].

[21] D. d. P. d. C. d. M. (DPCM), *Guidelines for the Assessment and the Reduction of the Seismic Risk of Cultral Heritage,* Rome, Italy: Gazzetta Ufficiale, 2011.

[22] S. Tesfamaraim and M. Saatcioglu, "Seismic risk assessment of RC building using fuzzy synthetic evaluation," *Journal of Earthquake Engineering,* vol. 12, no. 7, pp. 1157-1184, 2008.

[23] X. Romão and E. Paupério, "An indicator for post-disaster economic loss valuation of impacts on cultural heritage," *International Journal of Architectural Heritage,* pp. 1-20, 2019.

[24] L. A. Zadeh, "Fuzzy sets," *Information and control,* vol. 8, no. 3, pp. 338-353, 1965.

[25] G. Proietti, "Dopo la polvere". Rilevazione degli interventi di recupero (1985-1989) del patrimoni artistico-monumentale danneggiato dal terremoto del 1980-1981, Roma: Istituto Poligrafico e Zecca dello Stato, 1994.

[26] F. Doglioni, "Codice di pratica (Linee Guida) per la progettazione degli interventi di riparazione, miglioramento sismico e restauro dei beni architettonici danneggiati dal terremoto umbro-marchigiano del 1997," *Bollettino Ufficiale Regione Marche,* vol. 15, 2000.

[27] G. P. Cimellaro, I. P. Christovasilis, A. M. Reinhorn, A. De Stefano and T. Kirova, "L'Aquila Earthquake of April 6, 2009 in Italy: Rebuilding a Resilient City to Withstand Multiple Hazards," MCEER, 2010.

[28] J. H. Pirenne and K. F. Wallace, Europe in Transition 1300–1520, Boston: Houghton Mifflin Company, 1963.

[29] W. C. Jordan, Europe in the Middle Ages, London: Penguin Books, 2002.

[30] A. Cagnana, "La transizione al Medioevo attraverso la storia delle tecniche murarie: dall'analisi di un territorio ad un problema sovraregionale," in *I Congresso Nazionale di Archeologia Medievale*, Pisa, 1997.

[31] G. Magenes and A. Penna, "Existing masonry buildings: general codes issues and methods of analysis and assessment.," *Eurocode,* vol. 8, pp. 185-198, 2009.

[32] D. Dowrick, Earthquake Resistant Design and Risk Reduction. Earthquake Resistant Design and Risk Reduction: Second Edition, Chichester, UK: John Wiley & Sons, Ltd, 2009.

[33] A. Parducci, Fondamenti di ingegneria sismica in 80 lezioni, Naples, Italy: Liguori Editore, 2011.

[34] The National Academies, Disaster Resilience: A National Imperative, Washington, D.C.: The National Academies Press, 2012.

[35] A. Basaglia, A. Aprile, E. Spacone and F. Pilla, "Performance-based seismic risk assessment of urban systems," *International Journal of Architectural Heritage,* vol. 12, no. 7-8, pp. 1131-1149, 2018.

[36] H. Frantzich, "Risk analysis and fire safety engineering," *Fire Safety Journal,* vol. 31, no. 4, pp. 313-329, 1988.

[37] J. C. Martinez, "Methodology for conducting discrete-event simulation studies in construction engineering and management," *Journal of Construction Engineering and Management,* vol. 136, no. 1, pp. 3-16, 2009.

[38] ACI Committee and International Organization for Standardization, Building code requirements for structural concrete (ACI 318-19), American Concrete Institute, 2019.

[39] G. De Matteis and M. Zizi, "Seismic Damage Prediction of Masonry Churches by a PGA-Based Approach," *International Journal of Architectural Heritage,* vol. 13, no. 7, p. 1165–1179, 2019.

[40] S. Lagomarsino, "On the vulnerability assessment of monumental buildings," *Bullettin of Earthquake Engineering,* vol. 4, no. 4, pp. 445-463, 2006.

[41] S. Lagomarsino and S. Giovinazzi, "Macroseismic and mechanical models for the vulnerability and damage assessment of current buildings," *Bulletin of Earthquake Engineering,* vol. 4, no. 4, pp. 415-443, 2006.

[42] N. Chieffo and A. Formisano, "Geo-hazard-based approach for the estimation of seismic vulnerability and damage scenarios of the old city of senerchia (Avellino, Italy)," *Geosciences,* vol. 9, no. 2, p. 59, 2019.

[43] A. N. Rovida, M. Locati, R. D. Camassi, B. Lolli and P. Gasperini, "CPTI15, the 2015 version of the Parametric Catalogue of Italian Earthquakes," INGV (Istituto Nazionale di Geologia e Vulcanologia), 2016.

[44] E. Cosenza and G. Manfredi, "Damage indices and damage measures," *Progress in Structural Engineering and Materials,* vol. 2, no. 1, pp. 50-59, 2000.

[45] M. Zucconi, R. Ferlito and L. Sorrentino, "Validation and extension of a statistical usability model for unreinforced masonry buildings with different ground motion intensity measures," *Bulletin of Earthquake Engineering,* vol. 18, no. 2, pp. 767-795, 2020.

[46] MIT and CSLP, "Spettri NTC," 8 May 2020. [Online]. Available: http://cslp.mit.gov.it/index.php?option=com_content&task=view&id=75&Itemid=20. [Accessed 23 September 2020].

[47] *Norme Tecniche per le Costruzioni,* 2018.

[48] Technical Committee BD-006, NZS 1170.5:2004 - Structural Design Actions. Part 5: Earthquake Actions - New Zealand, 2004.

[49] A. S. o. C. E. (ASCE) and S. E. I. (SEI), *ASCE/SEI 7-16: Minimum Design Loads and Associated Criteria for Buildings and Other Structures,* 2016.

[50] A. Giuffrè, "Philological restoration of historical monuments. The cathedral of "Sant'Angelo dei Lombardi" in Irpinia," in *Structural conservation of stone masonry. International technical conference*, Athens, 1989.

[51] A. Marotta, S. Sorrentino, D. Liberatore and J. M. Ingham, "Vulnerability Assessment of Unreinforced Masonry Churches Following the 2010-2011 Canterbury Earthquake Sequence," *Journal of Earthquake Engineering,* vol. 21, no. 6, pp. 912-934, 2017.

[52] F. Gàlvez, S. R. Abeling, K. Ip, S. Giovinazzi, D. Dizhur and J. M. Ingham, "Using the Macro-element Method to Seismically Assess Complex URM Buildings," in *10th Australian Masonry Conference*, Sydney, 2018.

[53] S. Lagomarsino, S. Podestà, G. Cifani and A. Lemme, "The 31st October 2002 earthquake in Molise (Italy): a new methodology for the damage and seismic vulnerability survey of churches," in *Proceedings of the 13th World Conference on Earthquake Engineering*, Vancouver, BC, Canada, 2004.

[54] G. De Matteis, V. Corlito, M. Guadagnuolo and A. Tafuro, "Seismic Vulnerability Assessment and Retrofitting Strategies of Italian Masonry Churches of the Alife-Caiazzo Diocese in Caserta," *International Journal of Heritage Architecture,* pp. 1-16, 2019.

[55] Regione Lazio, "Tariffa dei Prezzi (Lavori Pubblici)," 2012. [Online]. Available: http://www.regione.lazio.it/binary/rl_main/tbl_documenti/INF_DGR_412_06_08_2012_Allegato3.pdf. [Accessed November 2019].

[56] Agenzia delle Entrate, "Banca dati delle quotazioni immobiliari," 2019. [Online]. Available: https://wwwt.agenziaentrate.gov.it/servizi/Consultazione/ricerca.htm. [Accessed September 2019].

[57] CCIAA, "Borsino Immobiliare," 2019. [Online]. Available: https://www.borsinoimmobiliare.it/. [Accessed September 2019].

[58] A. Benvenuti and M. Simonotti, "Incidenza dell'area in un segmento di mercato immobiliare," *Estimo e territorio,* vol. 12, 2005.

[59] S. Stanghellini, A. Mascarello and V. Ruaro, "La stima del valore di trasformazione: definizione e stima," 2009. [Online]. Available: http://www.iuav.it/Ateneo1/docenti/architettu/docenti-st/Stefano-St/archivio-p/CLASA-08-0/LEZIONI/La-stima-del-valore-di-trasformazione.pdf. [Accessed September 2019].

[60] M. Ciuna, "L'Allocation Method nella stima delle aree edificabile," *Aestimum,* vol. 57, no. 171, 2010.

[61] Made, "Come calcolare il valore di un terreno edificabile in pochi passi," 2018. [Online]. Available: https://ristrutturaconmade.it/come-calcolare-il-valore-di-un-terreno-edificabile/. [Accessed September 2019].

[62] J. White, Art and architecture in Italy 1250-1400, Yale University Press, 1993.

[63] M. A. Lavin, The place of narrative: mural decoration in Italian churches, 431-1600, University of Chicago Press, 1990.

[64] C. F. Altman, "The medieval marquee: Church portal sculpture as publicity," *The Journal of Popular Culture,* vol. 14, no. 1, pp. 37-46, 1980.

[65] J. Fitchen, The construction of Gothic cathedrals: a study of medieval vault erection., University of Chicago Press, 1981.

[66] Touring Club Italiano, Guide Rosse, Torino: Touring Club Italiano, From 1982 to 2015.

[67] T. Ross, Fuzzy logic with engineering applications, John Wiley & Sons, 2005.

[68] E. H. Mamdani, "Advances in the linguistic synthesis of fuzzy controllers," *International Journal of Man-Machines Studies,* vol. 8, no. 6, pp. 669-678, 1976.

[69] K. Pitilakis, H. Crowley and A. M. Kaynia, SYNER-G: Typology definition and fragility functions for physical elements at seismic risk: buildings, lifelines, transportation networks and critical facilities, vol. 27, Springer Science & Bus, 2014.

[70] A. J. Kappos, "An overview of the development of the hybrid method for seismic vulnerability assessment of buildings," *Structure and Infrastructure Engineering,* vol. 12, no. 12, pp. 1573-1584, 2016.

[71] E. Giuriani, Giuriani, E. 2012. Consolidamento Degli Edifici Storici, Turin, Italy: UTET, 2012.

[72] M. Vinci, Metodi di calcolo e tecniche di consolidamento per edifici in muratura., Palermo, Italy: Dario Flaccovio Editore, 2012.

[73] D. Pirchio, Unreinforced masonry Italian medievial churches: a holistic framework for the seismic risk assessment from the national scale to the building scale, South Bend, IN (US): Master's Thesis, University of Notre Dame, 2020.

[74] D. Pirchio, K. Q. Walsh, E. Kerr, I. Giongo, M. Giaretton, B. D. Weldon, L. Ciocci and L. Sorrentino, "Integrated framework to structurally model unreinforced masonry Italian medieval churches from photogrammetry to finite element model analysis through heritage building information modeling," *Engineering Structures,* vol. 241, no. 15, p. 112439, 2021.

[75] A. Borri and A. De Maria, "Il metodo IQM per la stima delle caratteristiche meccaniche delle murature: allineamento alla circolare n. 7/2019.," *ANIDIS,* pp. 2-21, 2019.

[76] W. Dong, Applications of Fuzzy Set Theory in Structural and Earthquake Engineering (Approximate Reasoning, Expert Systems), 1987.

[77] J. H. Tah and V. Carr, "A proposal for construction project risk assessment using fuzzy logic," *Constrution Management & Economics,* vol. 18, no. 4, pp. 491-500, 2000.

[78] M. Sánchez-Silva and L. Garcia, "Earthquake damage assessment based on fuzzy logic and neural networks," *Earthquake Spectra,* vol. 17, no. 1, pp. 89-112, 2001.

[79] E. S. Mistakidis and D. N. Georgiou, "Fuzzy sets in seismic inelastic analysis and design of reinforced concrete frames," *Advances in Engineering Software,* vol. 34, no. 10, pp. 589-599, 2003.

[80] S. Medasani, J. Kim and R. Krishnapuram, "An overview of membership function generation techniques for pattern recognition," *International Journal of approximate reasoning,* vol. 19, no. 3-4, pp. 391-417, 1998.

[81] I. Dikmen, M. T. Birgonul and S. Han, "Using fuzzy risk assessment to rate cost overrun risk in international construction projects," *International journal of project management,* vol. 25, no. 5, pp. 494-505, 2007.

[82] A. N. Whitehead, A treatise on universal algebra: with applications, Cambridge: Cambridge University Press, 1898.

## Index of the Figures

Figure 1 – Map of Italy indicating the nine dioceses in which churches were surveyed superimposed atop the national seismic hazard map. $PGA_{475}$ = peak ground acceleration for a 475-years average return period. Seismic zones adopted from the Italian National Civil Protection [20].

Figure 2 – Examples of prototypical churches surveyed: a) Santa Maria Assunta (Dasindo, Trentino – Alto Adige); b) San Matteo Apostolo (Cavazzale, Veneto); c) Santi Leonardo e Cristoforo (Monticchiello, Toscana); d) Sant'Ansano Martire (Petrignano del Lago, Umbria); e) Maddalena (Alatri, Lazio); f) Santa Maria di Casarlano (Casarlano, Campania).

Figure 3 – Typology, absolute number of churches, and relative number of churches surveyed categorized by floor plan and vault system.

Figure 4 – Normal distribution and relative frequency of the PGA corresponding to $PGA_{90}$, $PGA_{151}$, $PGA_{1424}$, and $PGA_{2475}$.

**Index of the Tables**

| # | Church Name | Region | Diocese | Settlement / City | Coordinates WGS84 GD | Role | Original Construction Year |
|---|---|---|---|---|---|---|---|
| 1 | Santi Dioniso, Rustico ed Eleuterio Martiri | Trentino – Alto Adige | Trento | Santa Croce | 46.066530 10.839030 | Parish church | 1155 |
| 2 | Santa Maria Assunta | Trentino – Alto Adige | Trento | Tavodo | 46.066530 10.893080 | Parish church | 1160 |
| 3 | San Giovanni Apostolo ed Evangelista | Trentino – Alto Adige | Trento | Poia | 46.028870 10.884130 | Parish church | 1200 |
| 4 | San Marcello | Trentino – Alto Adige | Trento | Lundo | 46.011910 10.884130 | Parish church | 1200 |
| 5 | Santa Maria Assunta | Trentino – Alto Adige | Trento | Dasindo | 46.010960 10.860530 | Subsidiary church | 1200 |
| 6 | San Lorenzo | Trentino – Alto Adige | Trento | Vigo Lomaso | 46.012050 10.872040 | Parish church | 1210 |
| 7 | San Nicolò | Trentino – Alto Adige | Trento | Comighello | 46.034260 10.849410 | Parish church | 1250 |
| 8 | Santa Maria Assunta e San Giovanni Battista | Trentino – Alto Adige | Trento | Tione | 46.034190 10.729450 | Parish church | 1300 |
| 9 | Annunciazione di Maria | Trentino – Alto Adige | Trento | Rango | 46.018330 10.811640 | Parish church | 1400 |
| 10 | San Felice | Trentino – Alto Adige | Trento | Bono | 46.026080 10.848670 | Parish church | 1480 |
| 11 | Santi Pietro e Paolo | Trentino – Alto Adige | Trento | Sclemo | 46.055610 10.882940 | Subsidiary church | 1490 |
| 12 | San Vigilio | Trentino – Alto Adige | Trento | Stenico | 46.052460 10.854170 | Parish church | 1500 |
| 13 | San Giorgio | Trentino – Alto Adige | Trento | Dorsino | 46.072690 10.896920 | Subsidiary church | 1500 |
| 14 | Santi Pietro e Paolo | Trentino – Alto Adige | Trento | Cares | 46.032700 10.866660 | Parish church | 1500 |
| 15 | San Biagio Vescovo e Martire | Trentino – Alto Adige | Trento | Favrio | 45.999920 10.858800 | Subsidiary church | 1500 |
| 16 | Sant'Antonio Abate | Trentino – Alto Adige | Trento | Bivedo | 46.028170 10.827460 | Parish church | 1530[2] |
| 17 | Immacolata e Santi Fabiano e Sebastiano | Trentino – Alto Adige | Trento | Fiavè | 46.004600 10.842050 | Parish church | 1540 (1880)[1] |
| 18 | Santa Maria Etiopissa | Veneto | Vicenza | Polegge | 45.605930 11.557180 | Subsidiary church | 1000 |
| 19 | Santa Maria e Santa Fosca | Veneto | Vicenza | Dueville | 45.634970 11.548010 | Parish church | 1050 (1955)[1] |
| 20 | Santa Maria Annunziata | Veneto | Vicenza | Poia | 45.530100 11.423720 | Parish church | 1300 |
| 21 | San Pietro Apostolo | Veneto | Vicenza | Monticello Conte Otto | 45.594130 11.585370 | Parish church | 1350 |
| 22 | Santa Margherita Vergine e Martire | Veneto | Vicenza | Posina | 45.790430 11.261480 | Parish church | 1400 |
| 23 | Santissima Trinità | Veneto | Vicenza | Bassano del Grappa | 45.724970 11.721980 | Parish church | 1400 |
| 24 | Santi Pietro e Paolo | Veneto | Vicenza | Nove | 45.724970 11.680790 | Parish church | 1440 |

| # | Church Name | Region | Diocese | Settlement / City | Coordinates WGS84 GD | Role | Original Construction Year |
|---|---|---|---|---|---|---|---|
| 25 | Santi Girolamo e Bernardino | Veneto | Vicenza | Vivaro | 45.610720 11.544320 | Parish church | 1460 |
| 26 | Santo Stefano Protomartire | Veneto | Vicenza | Lupia | 45.640930 11.608730 | Parish church | 1470 |
| 27 | San Matteo Apostolo | Veneto | Vicenza | Cavazzale | 45.600760 11.569250 | Parish church | 1480 |
| 28 | San Michele Arcangelo | Veneto | Vicenza | Sarmego | 45.599800 11.671670 | Parish church | 1500 |
| 29 | Santa Cristina | Veneto | Vicenza | Poianella | 45.632870 11.625320 | Parish church | 1560[2] |
| 30 | Beata Vergine di Monte Berico | Veneto | Vicenza | Vivaro | 45.621370 11.560270 | Subsidiary church | 1770[1] |
| 31 | San Secondiano | Toscana | Montepulciano – Chiusi - Pienza | Chiusi | 43.015560 11.949120 | Parish church | 550[1] |
| 32 | San Lorenzo | Toscana | Montepulciano – Chiusi - Pienza | Valiano | 43.148320 11.901600 | Parish church | 1100 |
| 33 | Santa Croce | Toscana | Montepulciano – Chiusi - Pienza | Abbadia San Salvatore | 42.880090 11.678360 | Parish church | 1100 |
| 34 | Santi Pietro e Paolo | Toscana | Montepulciano – Chiusi - Pienza | Petroio | 43.141490 11.688210 | Parish church | 1180 |
| 35 | Santi Leonardo e Cassiano | Toscana | Montepulciano – Chiusi - Pienza | San Casciano dei Bagni | 42.871630 11.875230 | Parish church | 1200 |
| 36 | Santissima Annunziata | Toscana | Montepulciano – Chiusi - Pienza | Montisi | 43.156690 11.651720 | Parish church | 1200 |
| 37 | San Francesco | Toscana | Montepulciano – Chiusi - Pienza | Chiusi | 43.016640 11.947110 | Parish church | 1210 |
| 38 | San Leonardo | Toscana | Montepulciano – Chiusi - Pienza | Montefollonico | 43.128120 11.745330 | Parish church | 1215 |
| 39 | San Pietro | Toscana | Montepulciano – Chiusi - Pienza | Radicofani | 42.896360 11.767490 | Parish church | 1220 |
| 40 | Santi Leonardo e Cristoforo | Toscana | Montepulciano – Chiusi - Pienza | Monticchiello | 43.068370 11.725680 | Parish church | 1300 |
| 41 | Sant'Apollinar e | Toscana | Montepulciano – Chiusi - Pienza | San Francesco | 43.016000 11.946030 | Subsidiary church | 1400 |
| 42 | San Vincenzo e Anasiasio | Toscana | Montepulciano – Chiusi - Pienza | Ascianello | 43.139580 11.797180 | Subsidiary church | 1450 |
| 43 | San Giovanni Battista | Umbria | Perugia – Città della Pieve | Castiglione della Valle | 43.018110 12.253970 | Parish church | 1100 |
| 44 | San Feliciano | Umbria | Perugia – Città della Pieve | San Feliciano | 43.119030 12.166770 | Parish church | 1170 |
| 45 | Sant'Ansano Martire | Umbria | Perugia – Città della Pieve | Petrignano del Lago | 43.148450 11.937900 | Parish church | 1190 |
| 46 | Crocifisso | Umbria | Perugia – Città della Pieve | Torgiano | 43.018380 12.437670 | Parish church | 1200 |
| 47 | San Martino di Fontana | Umbria | Perugia – Città della Pieve | Fontana | 43.113110 12.324470 | Parish church | 1300 |
| 48 | Santissimo Salvatore e Santa Maria Assunta | Umbria | Perugia – Città della Pieve | Paciano | 43.023420 12.070170 | Parish church | 1480 |
| 49 | San Lorenzo | Umbria | Perugia – Città della Pieve | Gioiella | 43.093580 11.971890 | Parish church | 1500 |
| 50 | Santa Maria delle Grazie | Umbria | Perugia – Città della Pieve | Montepetriolo | 43.016910 12.229730 | Subsidiary church | 1500 |

| # | Church Name | Region | Diocese | Settlement / City | Coordinates WGS84 GD | Role | Original Construction Year |
|---|---|---|---|---|---|---|---|
| 51 | Annunziata | Umbria | Perugia – Città della Pieve | Fontignano | 43.026540 12.191760 | Subsidiary church | 1500 |
| 52 | San Terenziano | Umbria | Orvieto - Todi | San Terenziano | 42.863510 12.471800 | Parish church | 1200 |
| 53 | Santi Giacomo e Marco | Umbria | Orvieto - Todi | Castel dell'Aquila | 42.633830 12.406490 | Parish church | 1200 |
| 54 | San Lorenzo Martire | Umbria | Orvieto - Todi | Montegiove | 42.917050 12.144030 | Subsidiary church | 1270 |
| 55 | San Biagio Vescovo e Martire | Umbria | Orvieto - Todi | Porano | 42.686550 12.101730 | Parish church | 1270 |
| 56 | Sant'Andrea Apostolo | Umbria | Orvieto - Todi | Marcellano | 42.872980 12.520790 | Parish church | 1300 |
| 57 | Santa Maria Assunta | Umbria | Orvieto - Todi | Montecchio | 42.663140 12.286270 | Parish church | 1300 |
| 58 | San Nicolò | Umbria | Orvieto - Todi | Farnetta | 42.648420 12.453280 | Parish church | 1400 |
| 59 | San Pancrazio Martire | Umbria | Orvieto - Todi | Castel Giorgio | 42.704710 11.979650 | Parish church | 1520[2] |
| 60 | Maddalena | Lazio | Anagni-Alatri | Alatri | 41.716550 13.352380 | Subsidiary church | 1100 |
| 61 | Santa Maria Maggiore | Lazio | Anagni Alatri | Alatri | 41.726150 13.342160 | Parish church | 1100 |
| 62 | Santa Maria al Colle | Lazio | Anagni Alatri | Fiuggi | 41.804120 13.218100 | Parish church | 1200 |
| 63 | Santi Nicola e Giovanni | Lazio | Anagni Alatri | Filettino | 41.889500 13.319210 | Subsidiary church | 1200 |
| 64 | Sant'Antonio | Lazio | Anagni Alatri | Filettino | 41.890270 13.328870 | Subsidiary church | 1274 |
| 65 | San Michele Arcangelo e San Gaurico | Lazio | Anagni Alatri | Fumone | 41.727160 13.290440 | Parish church | 1350 |
| 66 | Santa Maria Maddalena | Lazio | Palestrina | Capranica Prenestina | 41.862310 12.952400 | Parish church | 1400 |
| 67 | Santissima Annunziata | Campania | Sorrento – Castellammare di Stabia | Vico Equense | 40.663880 14.423930 | Subsidiary church | 1330 |
| 68 | San Renato Vescovo | Campania | Sorrento – Castellammare di Stabia | Moiano | 40.650660 14.466020 | Parish church | 1340 |
| 69 | Santa Maria Assunta | Campania | Sorrento – Castellammare di Stabia | Vico Equense | 40.655540 14.435040 | Subsidiary church | 1400 |
| 70 | Santa Maria di Casarlano | Campania | Sorrento – Castellammare di Stabia | Casarlano | 40.623250 14.391680 | Parish church | 1425 |
| 71 | San Giovanni Evangelista | Campania | Sorrento – Castellammare di Stabia | Vico Equense | 40.662960 14.436400 | Parish church | 1490 |
| 72 | Sant'Antonio | Campania | Nocera Inferiore - Sarno | Nocera Inferiore | 40.746980 14.645720 | Parish church | 1260 |

[1]The church was selected beyond specific request of the diocese.

[2]Although the original construction year is slightly outside of the selected limits, the church was selected because it was respecting the other criteria.

*Table A 1 – Selected churches*

## Appendix B: Indices of Risk Subcomponent

### *Hazard*

The resulting indices of hazard $i_{H,i}$ are shown in Figure B 1 subdivided based on the considered return period scenario and sorted by region.

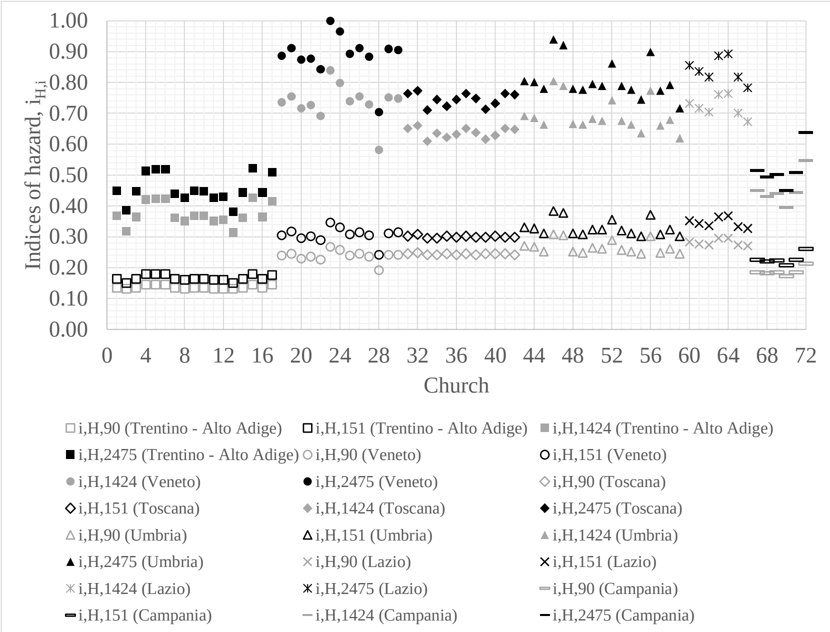


*Figure B 1 – Indices of hazard* $i_{H,i}$ *designated by the considered return period scenario and sorted by region.*

### *Vulnerability*

The resulting indices of vulnerability $i_{V,i}$ are shown in Figure B 2 subdivided based on the considered scenario and sorted by region. As can be expected the indices vary over a wide range, given the intrinsic variability in building structural features.

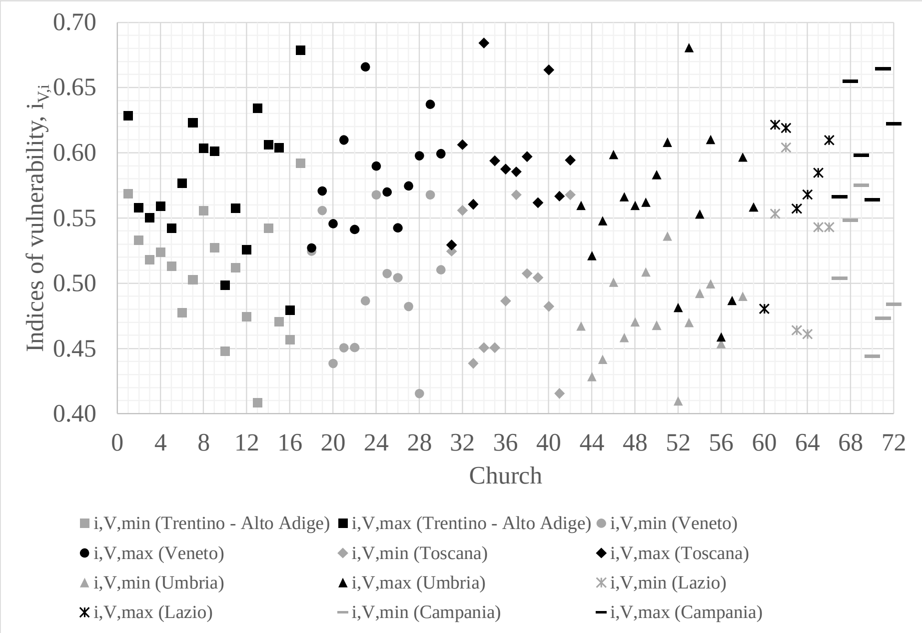


*Figure B 2 – Indices of vulnerability* $i_{V,i}$ *designated by the considered vulnerability scenario (min or max) and sorted by region.*

## ***Exposure***

### *Occupancy Rate*

The resulting indices of occupancy rate $i_{OR,i}$ are shown in Figure B 3 subdivided based on the considered scenario and sorted by region.

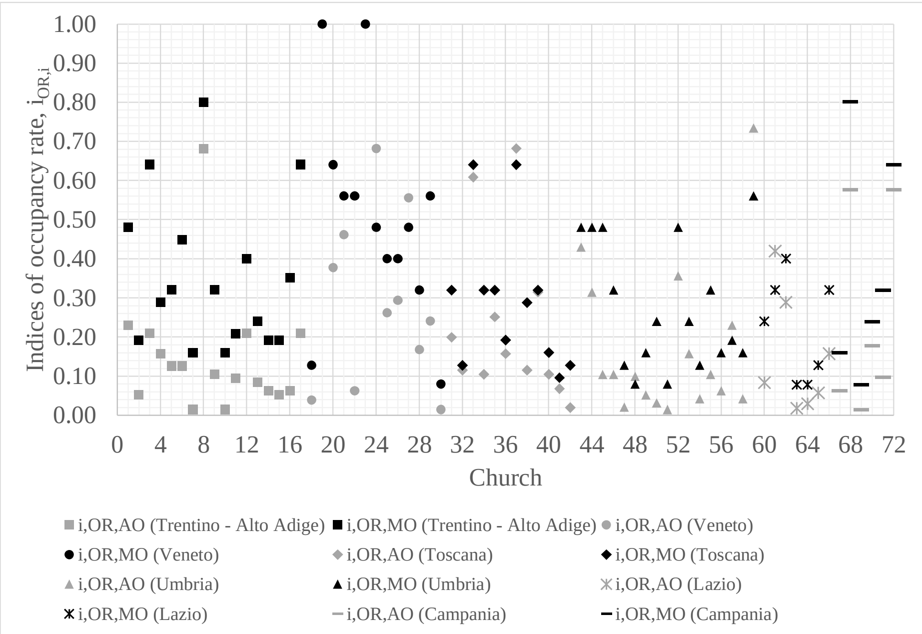


*Figure B 3 – Indices of occupancy rate* $i_{OR,i}$ *designated by the considered scenario and sorted by region.*

*Cummunity Use*

The resulting indices of community use $i_{CU,i}$ are shown in Figure B 4 subdivided based on the considered scenario and sorted by region.

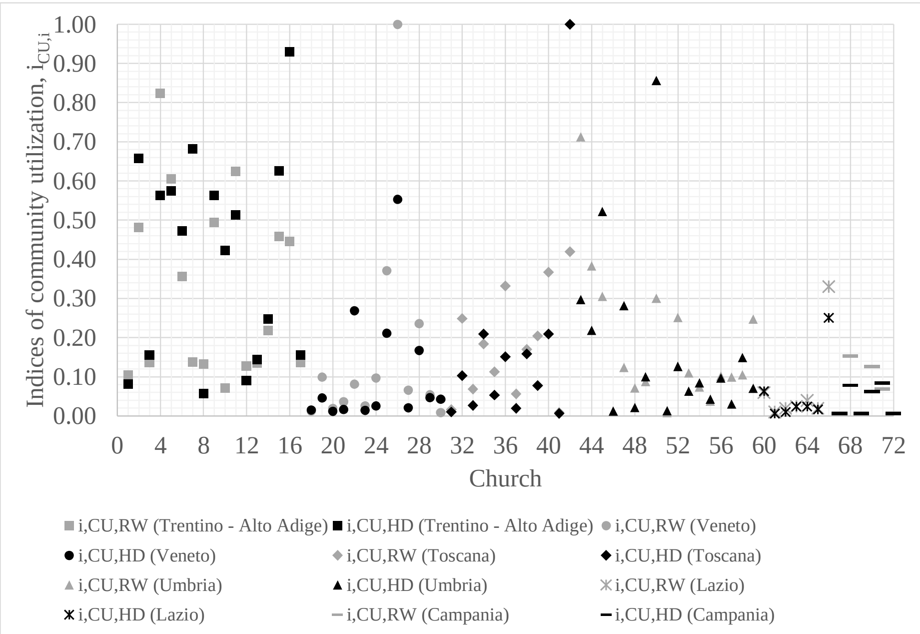


*Figure B 4 – Indices of community use $i_{CU,i}$ designated by the considered scenario and sorted by region.*

***Consequences***

*Equivalent Economic Value*

The resulting indices of equivalent economic value $i_{EEV,i}$ are shown in Figure B 5 subdivided based on the considered scenario and sorted by region.

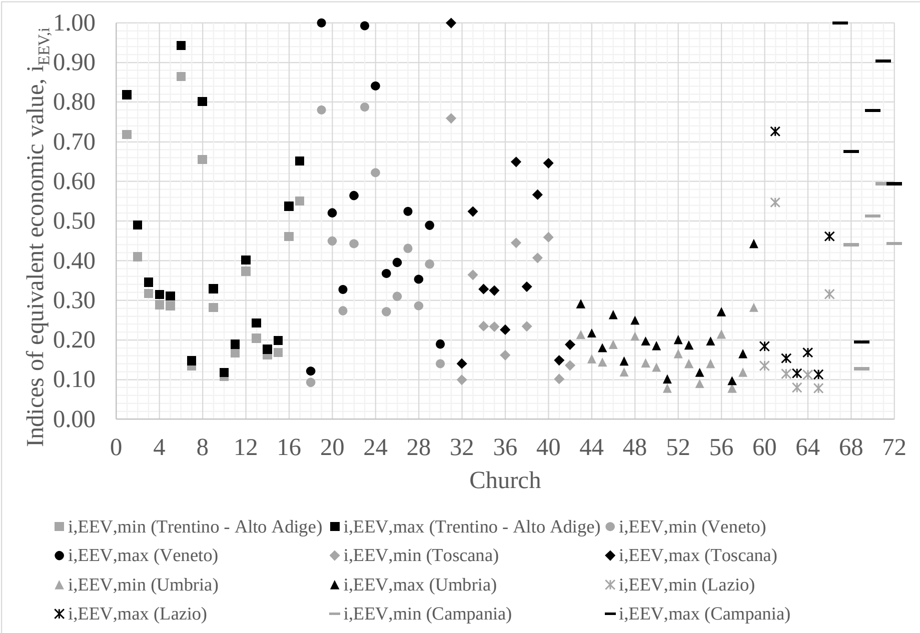


*Figure B 5 – Indices of equivalent economic value $i_{EEV,i}$ designated by the considered scenario and sorted by region.*

*Susceptible Heritage*

The resulting indices of susceptible heritage $i_{SH,i}$ are shown in Figure B 6 sorted by region.

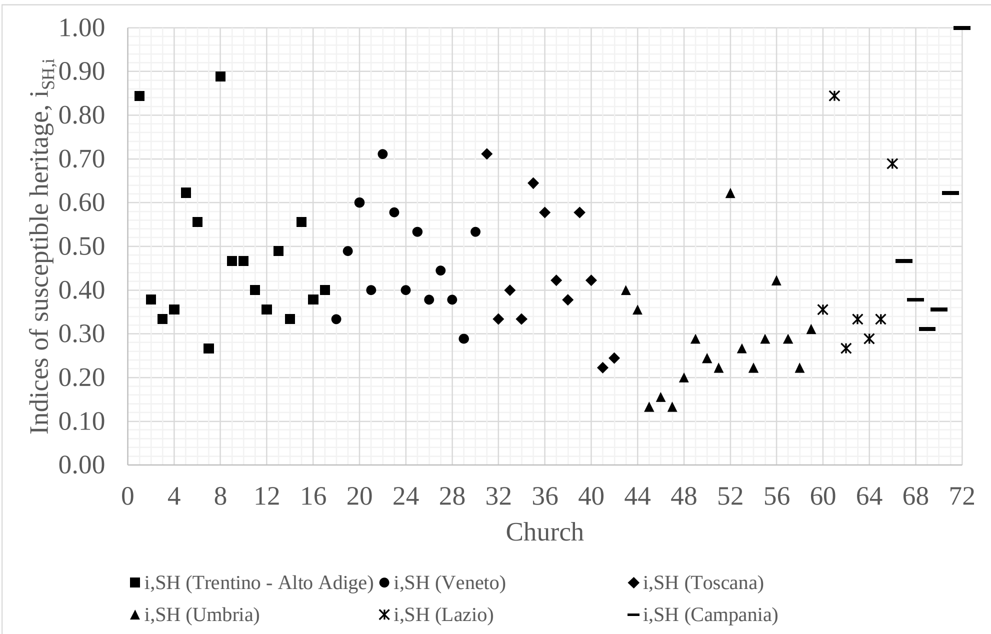


*Figure B 6 – Indices of susceptible heritage $i_{SH,i}$ designated by the considered scenario and sorted by region.*

## Appendix C: Criteria to determine $I_{i,ki}$ and $I_{e,kp}$

Given the subjectivity of the criteria to determine the score for the vulnerability indicators and the robustness improvers, $v_{ki}$ and $v_{kp}$, more extensive criteria were developed to address the influence score of the vulnerability indicators, $I_{e,kp}$, and the effectiveness score of the robustness improvers, $I_{i,ki}$, of the selected churches. The authors underline that the applied criteria were developed for the purposes of a rapid and effective visual survey, based on the recurrent characteristics of the analyzed churches. The criteria might still have a subjective component and further research to achieve more scientific criteria would be desirable.

Whenever uncertainties regarding the assessment of any macro-block occurred (due to impossibility of accessing directly the element, or to the difficulty of establishing a correct score) a conservative approach was applied by considering both the worst and the best-case scenario. While the application of the criteria is related to the correspondent collapse mechanism of each macro-block in **Errore. L'origine riferimento non è stata trovata.**Table C 1, a description of each criterion is listed in Table C 2 and Table C 3.

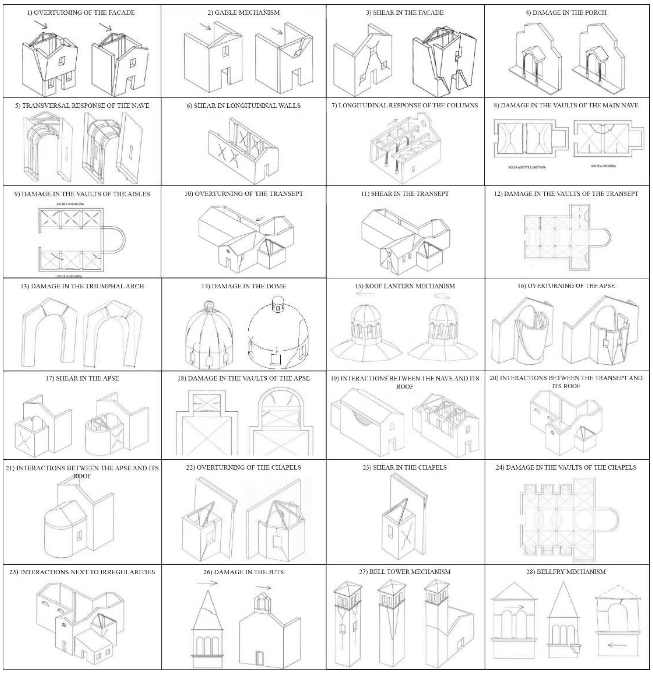


*Figure C 1 – Collapse mechanisms [21].*

| Macro-block (Errore. L'origine riferimento non è stata trovata.) | Collapse Mechanism (Figure C 1) | Criteria applied for vulnerability indicators | Criteria applied for robustness improvers |
|---|---|---|---|
| Façade | 1) Overturning of the façade | V1; V2 | R1; R2; R3 |
| | 2) Gable mechanism | V2; V3; V4 | R4; R5; R6 |
| | 3) Shear in the façade | V2; V5 | R1; R7 |
| | 4) Damage in the porch | V1 | R1; R8 |
| Lateral Walls | 5) Transversal response of the nave | V1; V5 | R1; R2; R7 |
| | 6) Shear in the longitudinal walls | V2; V5 | R6; R9; R10 |
| Nave | 7) Longitudinal response of the columns | V1; V6 | R1; R2 |
| | 8) Damage in the vaults of the main nave | V7; V8; V9 | R1; R2 |
| | 9) Damage in the vaults of the aisles | V7; V8; V9 | R1; R2 |
| Transept | 10) Overturning of the transept | V2; V3; V4 | R1; R2; R3; R4; R6 |
| | 11) Shear in the transept | V2; V4 | R6; R9; R10 |
| | 12) Damage in the vaults of the transept | V7; V8; V9 | R1; R2 |
| Triumphal Arch | 13) Damage in the triumphal arch | V1; V6 | R1; R7; R11 |
| Dome | 14) Damage in the dome | V7; V10 | R2; R12; R13 |
| | 15) Roof lantern mechanism | V5 | R2; R12; R14 |
| Apse | 16) Overturning of the apse | V1; V2; V4 | R2; R5; R12 |
| | 17) Shear in the apse | V2; V4 | R6; R9; R10 |
| | 18) Damage in the vaults of the apse | V7; V8; V9 | R1; R2 |
| Chapels | 22) Overturning of the chapels | V2 | R1; R2; R3 |
| | 23) Shear in the chapels | V2; V4 | R6; R9; R10 |
| | 24) Damage in the vaults of the chapels | V7; V8; V9 | R1; R2 |
| Projections | 26) Damage in the juts | V5; V11; V12 | R4; R9; R15 |
| Bell Tower | 27) Bell tower mechanism | V2; V13; V11 | R1; R3; R9; R16 |
| | 28) Belfry mechanism | V1; V6 | R1; R8; R17 |
| Interactions | 19) Interaction between the nave and its roof | V1; V4 | R4; R5; R6; R18 |
| | 20) Interaction between the transept and its roof | V1; V4 | R4; R5; R6; R18 |
| | 21) Interaction between the apse and its roof | V1; V4 | R4; R5; R6; R18 |
| | 25) Interaction next to irregularities | V7; V14 | R1; R19 |

*Table C 1 – Application of the criteria in Table C 2 and Table C 3 for the different collapse mechanisms of the macro-blocks*

| Criteria for the influence score of the vulnerability indicator, $I_{i,ki}$ | Description |
|---|---|
| V1: Thrusting elements | Thrusting elements will always exist when there are vaults, arches, or any element causing horizontal loading. The amount of the thrust would depend on the length of the span, the rise of the vault (or the arch), the overall geometry, the depth, and the composing material. However, in most cases only the span and rise can be quickly and |

| Criteria for the influence score of the vulnerability indicator, $I_{i,ki}$ | Description |
|---|---|
| | directly assessed and the intensity of the horizontal thrust can be estimated consequently. Thus, a scoring approach similar to V8 (long spans) was applied. |
| V2: Large openings | The presence of openings might significantly affect a masonry wall by creating a system of piers, instead of a solid wall behavior. A score of 5 might be assigned if the openings area (considering also their vertical projections) affect an area larger than the 50% of the area of the wall. A score of 4 might be assigned if the openings area (considering also their vertical projections) affect an area ranging between the 40% and the 50% of the area of the wall. A score of 3 might be assigned if the openings area (considering also their vertical projections) affect an area ranging between the 30% and the 40% of the area of the wall. A score of 2 might be assigned if the openings area (considering also their vertical projections) affect an area ranging between the 20% and the 30% of the area of the wall. A score of 1 might be assigned if the openings area (considering also their vertical projections) affect an area smaller than the 10% of the area of the wall. A score of 0 might be assigned only if the openings are absent or their dimension is negligible. |
| V3: Large and heavy groin/rib vault panels | This criterion has several similarities with V1 (thrusting elements) and it was assessed in a similar way. |
| V4: Stiff ring-beam | Stiff ring-beams exist where there is a concrete bond beam. This may or may not be visible. Roof retrofits that involve reinforced concrete provide a stiff ring-beams. There may be a reinforced concrete beam around the roof elements. Tell-tale marks of the presence of a reinforced concrete ring-beams might be noticed from the outside of the church. If joists are not visible outside the wall and the latter is plastered, then it might be tentatively assumed a concrete ring-beam is existing. A score of 5 might be assigned if there is a concrete ring-beam. The score should be lowered basing on the divergence from the worst-case scenario. |
| V5: Slenderness | The slenderness of an element negatively affects the out-of-plane performance. Given the difficulty of measuring directly the thickness of several macro-blocks, the score was based on the perceived geometry of the element. |
| V6: Excessively stiff or heavy roof | A stiff or heavy roof exists where there is a concrete roof or masonry vaults. A score of 5 might be assigned if there is a concrete roof or masonry vaults. A score not lower than 2 should be assigned for this criterion, unless the entire roof system (roof covering included) is constructed in timber and the connections can be assumed as effective. |
| V7: Concentrated loads | A large concentrated load might likely negatively affect the response of the loaded element by creating a "punching load" effect. Furthermore, the position might affect the distribution of the load towards the support. Asymmetric loads might cause an unequal loading of the supports and differential responses. A score of 5 might be assigned to large and asymmetric concentrated loads. The score should be lowered basing on the divergence from the worst-case scenario. |
| V8: Span length of arches/vaults | This criterion is associated with the presence of vaults or arches. A score of 5 might be assigned to span longer than 8 m. A score of 4 might be assigned to spans with length ranging between 6 and 8 m. A score of 3 might be assigned to spans with length ranging between 4 and 6 m. A score of 2 might be assigned to spans with length ranging between 2 and 4 m. A score of 1 might be assigned to spans shorter than 2 m. |
| V9: Irregular profile | Any asymmetry in the geometry of a vault (or an arch) might cause an increasing bending moment on the section, while arches are designed to take compressive stresses. The score was based on the perceived irregularity in the geometry of the vault (or arch). |
| V10: Large openings in the dome drum | This criterion has several similarities with V2 (large openings) and it was assessed in a similar way. |
| V11: False supports | False support might happen when a secondary element is not resting on a structural element, such as a load bearing wall, or on appropriate foundations system. A score of 0 might be assigned if the element is fully supported by a vertical bearing element or |

| **Criteria for the influence score of the vulnerability indicator, $I_{i,ki}$** | **Description** |
|---|---|
| | if it lays on its own foundations. The score should be increased basing on the divergence from the best-case scenario. |
| V12: Eccentric position | Secondary elements that are not symmetrically resting on primary vertical bearing elements might cause a differential response of the supports. A score of 0 might be assigned to elements that are symmetrical resting on the primary bearing element with respect both to the depth and the length. The score should be increased basing on the divergence from the best-case scenario. |
| V13: Asymmetric position of the bell tower | An asymmetric position of the bell tower coupled with a very stiff roof strongly connected to walls may lead to increased torsional action within the structure. A score of 0 might be assigned if the bell tower is properly separated from the church. The score should be increased basing on the divergence from the optimal scenario. |
| V14: Stiffness differences | Stiffness differences might exist if a structure or element that is either incorporated into the structure of the church or next to the church is of a different height and/or width and/or material. A score of 5 might be assigned if the two structures (i.e., the church and the considered irregularity) have significant differences in terms of material and geometry. The score should be lowered basing on the divergence from the worst-case scenario. |

*Table C 2 – Criteria for the influence score of the vulnerability indicator, $I_{i,ki}$*

| **Criteria for the effectiveness score of the robustness improver, $I_{e,kp}$** | **Description** |
|---|---|
| R1: Tie rods | For being fully effective tie rods must: 1) span in the direction perpendicular to the macroblock motion at location (height) that is effective for resisting motion, and 2) must extend through exterior walls or the member that it is supporting. If a tie rod exists in a direction that is not perpendicular to the macroblock motion or not providing restraint to motion of the specific element, then the tie rod may be considered absent for that category. If there is no evidence of a tie rod extending through a wall or member in which it is supporting, then it is not very effective. Also, look for signs of weakness or damage in the tie rod that may impact the effectiveness. Additonally, consider spacing between tie rods and size of the wall anchor. A score of 5 might be assigned if the criterion is fully respected. The score should be lowered basing on the divergence from the optimal scenario. |
| R2: Buttresses | Elements other than traditional buttresses may act as a buttress on an element of the structure. To be effective, buttresses must be providing resistance in the direction in which the macro-block needs support for. An element also needs to transfer loads into the foundation (or in the closest vertical bearing element) in order to be acting as a buttress. This may exist as another component of the church. There may be instances where a chapel serves as a buttress to the main nave or the aisle. To be serving as a buttress, the element must be interlocked as a component of the structure/element in which it is supporting. A score of 5 might be assigned if the buttresses are uniformly distributed along the direction of the vault, or at the exact position of the arches, and if the footprint is large enough to accommodate the inclined forces coming from the thrusting elements. The score should not be larger than 2 if there are buttresses just on one side of the thrusting element. The score should be lowered basing on the divergence from the optimal scenario. |
| R3: Connection to lateral walls | The criterion depends on how well connected the walls that are subject to overturning are connected to the walls perpendicular to them. For example, the façade and transept would both have some type of connection to a lateral wall. A well-connected lateral |

| Criteria for the effectiveness score of the robustness improver, $I_{e,kp}$ | Description |
|---|---|
| | wall means that the masonry is interlocked as a consequence of dressed units and staggered head joints. The mortar should also be strong and in good condition for full effectiveness. A lateral wall that would not be well connected would be a wall that does not have interconnected masonry blocks. Hooping elements or diagonal tie rods crossing the connecting walls increase the effectiveness of the connection. A score of 5 might be assigned if the criterion is fully respected. The score should not be larger than 4 if the connection is only based on masonry bond. The score should be lowered basing on the divergence from the optimal scenario. |
| R4: Connection to roof | All churches will have some type of connection to the roof. Newly renovated roofs will likely have a stronger connection and a score of 4 or 5 can be assigned in some instances. It is possible that newly renovated roofs in some churches were only renovated over certain sections of the church and may not include chapels, the apse, or transepts. Be certain that the entire roof has been retrofitted before giving all elements a full effective score for roof connections. A score of 5 might be assigned if devices to increase the effectiveness of the connection are applied (e.g., steel bars drilled in the bond beam and resins-filled holes). The score should not be larger than 3 if the connection between the roof and the vertical bearing elements is mainly based on friction. The score should be lowered basing on the divergence from the optimal scenario. |
| R5: Braced roof pitch | The braced roof pitch exists when there are adequate bracing elements connecting the roof frames. The more bracing there are, and the shorter the span between the bracing is, the more effective the braced roof pitch will be. This may not be visible. A score of 4 might be assigned if the roof is composed of concrete beams and a collaborating concrete slab, and a score of 5 if a lighter and properly designed bracing system is connecting the roof beams. The score should not be larger than 2 if a single layer of timber board is overlapped transversely to the roof beams. The score should be lowered basing on the divergence from the optimal scenario. If it is not something visible from inside the church, a conservative score of 0 might be assumed. |
| R6: Light ring-beam | The ring-beam should be light (timber, steel, reinforced masonry or FRP stripes), continuous, and well-connected to the vertical bearing element. A score of 5 might be assigned if the criterion is fully respected. The score should not be larger than 3 if the ring-beam is not continuous or if the connection with the vertical bearing element is mainly based on friction. In newly renovated roofs, a concrete beam may exist to ensure (if properly designed) a stronger connection between the roof and other building components. In this case, even though the connections are strong, the ring-beam is still heavy and stiff, and a score of 0 might be assigned. |
| R7: Lateral restraints | The criterion refers to components (other than buttresses) that are serving as lateral restraints. These components are not always part of the church structure and may not have a structural attachment. Lateral restraints of transverse motion may be in the form of surrounding structures that abut the element. Lateral restraints may also be interior elements that are not structural, but that may help to prohibit motion in direction specified in each category of the specified element. A score of 5 might be assigned if the lateral restraints are continuously restraining the transversal motion. The score should not be larger than 2 if there are lateral restraints just on one side of the thrusting element. The score should be lowered basing on the divergence from the optimal scenario. |
| R8: Columns dimension | This is only applicable for churches that have columns. Columns that are only located integral with lateral walls in a church that only has a main nave and no aisles are not considered in this criterion. The dimensions refer to how thick they are with respect to the height and span length of arch(es) converging into them. A score of 5 might be assigned if the footprint is large enough to accommodate the inclined forces coming from the thrusting elements. The score should be lowered basing on the divergence from the optimal scenario. |

| Criteria for the effectiveness score of the robustness improver, $I_{e,kp}$ | Description |
|---|---|
| R9: Quality of masonry | For the purposes of this criterion, the quality of the masonry is based on the qualitative approach of the masonry quality index [75]. The score for this criterion can be 1, 2, or 3 and equation 8 should be changed with $v_{kp,i} = \frac{I_{e,kp,R9}}{n_{kp}} + \frac{3}{5n_{kp}} \sum_{j=1}^{n_{kp}-1} I_{e,kp,j}$. A score of 3 might be assigned to a corresponding to masonry category "A" in the in-plane direction. A score of 2 might be assigned to a corresponding to masonry category "B" in the in-plane direction. A score of 1 might be assigned to a corresponding to masonry category "C" in the in-plane direction. The score should not be larger than 1 if the wall has extensive cracks. |
| R10: Lintels | Lintels should either look like beams, stonework, or brickwork around openings. These must be in good shape to transfer loads appropriately through masonry walls. A score of 5 might be assigned if the lintel has a properly large support on the vertical bearing elements surrounding the opening and no cracks are evident on the lintels or on the immediately surrounding area. The score should be lowered basing on the divergence from the optimal scenario. If any evidence of the absence of lintels might be noticed (extensive cracks surrounding the openings) a score of 0 might be assigned. |
| R11: Large thickness | This criterion refers to how thick triumphal arch is with respect of its length. The score was based on the perceived geometry of the triumphal arch. |
| R12: Radial bracing | This criterion has several similarities with R1 (tie rods). The main difference is the radial distribution of the tie rods to counteract the transversal forces. Also steel, timber, or FRP hooping members should be considered in this criterion and, if they exist, a score of 5 might be assigned. |
| R13: Connection to the triumphal arch | This criterion has several similarities with R4 (connection to roof) and it was assessed in a similar way. |
| R14: Lantern dimension | This criterion refers to the dimension of the lantern above the dome. The bigger the lantern is, the larger would be the load on the dome. Furthermore, slender lanterns could be likely affected by overturning. Given the difficulty of accessing the lantern directly, the score was based on the perceived geometry of the element. |
| R15: Elements dimension | This criterion has several similarities with R14 (lantern dimension) and it was assessed in a similar way. |
| R16: Distance of the bell tower from church walls | If the bell tower is not integral with the church or adjacent the actual church structure, then it will have some distance from the church. It may still be adjacent another structure that may be adjacent to the church, but not the church itself. A score of 5 might be assigned if there are no forms of connections between the bell tower and the church, and the minimum distance between the two structure is larger H/100, where H is the height of the church wall adjacent to the bell tower. The score should be lowered based on the divergence from the optimal scenario. |
| R17: Span length of the belfry arches | Short span arches provide better support than longer span arches. This is applicable if there are one or more arches in the belfry. Given the difficulty of accessing the belfry of each church, the score was based on the perceived geometry of the arch. A score of 5 might be assigned if the arch span was less than one third of the horizontal dimension of the belfry. The score should be lowered basing on the divergence from the optimal scenario. |
| R18: Connection to bond beams | This criterion has several similarities with R4 (connection to roof) and it was assessed in a similar way. |
| R19: Connection with later interventions | This criterion exists if there is a connection between the irregularity (other buildings typically) and the church structure. It has several similarities with R3 (connection to lateral walls) and it has been assessed in a similar way. If there is not clear integral connection, a score of 0 might be assigned. For example, if the other building/structure has a clear vertical joint without stones or bricks going into both the church and the |

| Criteria for the effectiveness score of the robustness improver, $I_{e,kp}$ | Description |
|---|---|
| | other structure (i.e., two distinct construction phases can be clearly recognized) A score of 5 might be assigned if there is no connection between the church and the other building/structure, and structural breaks were interposed between the two structures. |

861 *Table C 3 – Criteria for the effectiveness score of the robustness improver, $I_{e,kp}$.*

## Appendix D – Fuzzy Set Theory

***Step 1: Membership Ratio and Fuzzification of the Inputs***

Accordingly with previous research [76, 77, 78, 79, 22, 13], the sets $A_i$ were defined as risk categories related with the different components of risk. Five membership ratio elements (corresponding to 5 risk categories) were used to aggregate the probabilistic range of risk variables: VL (Very Low), L (Low), M (Medium), H (High), and VH (Very High). Therefore, the input risk subcomponents (e.g., $i_{H,90}$) were "fuzzified" into a five-tuple $\mu_i = [\mu_{VL,i} ; \mu_{L,i} ; \mu_{M,i} ; \mu_{H,i} ; \mu_{VH,i}]$ known as the membership ratio set wherein each element represents the sensitivity of the variable value to each category from VL to VH. The membership ratio can be assigned following different methods [67, 80]; however, only the "Heuristic Method" was used to define the membership ratio set $\mu_i$ since it is commonly applied for engineering risk assessment [13, 22]. The heuristic method defines each set using a "Triangular Fuzzy Number" (TFN). The TFN is characterized by a three-tuple array $TFN^j = [a_1^j; a_2^j; a_3^j]$ where $a_1^j$, $a_2^j$, and $a_3^j$ represent, respectively, where the membership to the given *j*-th set starts, reaches its maximum, and ends (with $j = VL, L, M, H, VH$). Thus, the membership ratio can be determined in accordance with Equation D 1.

$$\mu_i{}^j{}_{(i_i)} = \begin{cases} 0, & i_i \le a_1{}^j \\ \frac{i_i - a_1{}^j}{a_2{}^j - a_1{}^j}, & a_1{}^j < i_i \le a_2{}^j \\ \frac{a_3{}^j - i_i}{a_3{}^j - a_2{}^j}, & a_2{}^j < i_i \le a_3{}^j \\ 0, & i_i > a_3{}^j \end{cases} \tag{D 1}$$

where: $i_i$ is the index related to the $i$-th risk component;

$\mu_i{}^j{}_{(i_i)}$ is the $j$-th component of the fuzzified five-tuple array corresponding to the index $i_i$;

$a_1{}^j$, $a_2{}^j$, and $a_3{}^j$ are the components of $TFN^j$.

The values of $TFN^j$ are shown in Table D 1.

| SET | Very Low [VL] | Low [L] | Medium [M] | High [H] | Very High [VH] |
|---|---|---|---|---|---|
| Triangular Fuzzy Number | $TFN^{VL}$ [0; 0; 0.25] | $TFN^{L}$ [0; 0.25; 0.5] | $TFN^{M}$ [0.25; 0.5; 0.75] | $TFN^{H}$ [0.5; 0.75; 1] | $TFN^{VH}$ [0.75; 1; 1] |

*Table D 1– Triangular fuzzy numbers (TFN) of the membership ratio.*

Similarly to Sanchez-Silva and Garcia [78], Dickmen, Nirgonul and Han [81], and Tesfamaraim and Saatcioglu [22], five sets (i.e., VL, L, M, H, and VH), instead of three [13], were considered to avoid an excessive discretization of the results. The indices of risk components were fuzzified using Equation D 1.

***Step 2: Aggregation of two five-tuple sets***

According to Mamdani [68] and Zadeh [24], two five-tuple sets can be combined into a resulting five-tuple set using a procedure called "aggregation" by Ross [67]. Thus, to result in one single seismic risk rating, 13 five-tuple sets (determined starting from the risk subcomponents) were aggregated in couples until one single five-tuple set remained. Since the aggregation is commutative, the order of aggregation is irrelevant. The aggregation of the components of two five-tuple sets $\mu_1 = [\mu_{VL,1}; \mu_{L,1}; \mu_{M,1}; \mu_{H,1}; \mu_{VH,1}]$ and $\mu_2 = [\mu_{VL,2}; \mu_{L,2}; \mu_{M,2}; \mu_{H,2}; \mu_{VH,2}]$ should be based on rules $r^k$ that combine the two five-tuple sets' components into a single aggregated five-tuple set $\mu_r = [\mu_{VL,r}; \mu_{L,r}; \mu_{M,r}; \mu_{H,r}; \mu_{VH,r}]$. Since each five-tuple set μi has five components, each set of rules rk was constituted of 25 elements ($k$ = [1, 2, 3, …, 25]), accounting for any possible combination as shown in Table D 2.

| Rule Set [r] | Set input 1 [$\mu_1{}^{ik}$] | Set input 2 [$\mu_2{}^{jk}$] | Set output [$\mu_r{}^{j}$] | Rule Set [r] | Set input 1 [$\mu_1{}^{ik}$] | Set input 2 [$\mu_2{}^{jk}$] | Set output [$\mu_r{}^{j}$] |
|---|---|---|---|---|---|---|---|
| $r^1$ | VL | VL | VL | $r^{14}$ | M | H | H |
| $r^2$ | VL | L | L | $r^{15}$ | M | VH | H |
| $r^3$ | VL | M | L | $r^{16}$ | H | VL | M |
| $r^4$ | VL | H | M | $r^{17}$ | H | L | M |

| Rule Set [r] | Set input 1 [$\mu_1^{jk}$] | Set input 2 [$\mu_2^{jk}$] | Set output [$\mu_r^j$] | Rule Set [r] | Set input 1 [$\mu_1^{jk}$] | Set input 2 [$\mu_2^{jk}$] | Set output [$\mu_r^j$] |
|---|---|---|---|---|---|---|---|
| $r^5$ | VL | VH | M | $r^{18}$ | H | M | H |
| $r^6$ | L | VL | L | $r^{19}$ | H | H | H |
| $r^7$ | L | L | L | $r^{20}$ | H | VH | VH |
| $r^8$ | L | M | M | $r^{21}$ | VH | VL | M |
| $r^9$ | L | H | M | $r^{22}$ | VH | L | H |
| $r^{10}$ | L | VH | H | $r^{23}$ | VH | M | H |
| $r^{11}$ | M | VL | L | $r^{24}$ | VH | H | VH |
| $r^{12}$ | M | L | M | $r^{25}$ | VH | VH | VH |
| $r^{13}$ | M | M | M | | | | |

*Table D 2 – Combination rules $r^k$.*

The combinations in Table D 2 are resolved by means of the Boolean rule of set intersection [82] in Equation D 2:

$$[\mu_r{}^j]_k = \mu_1{}^{jk} \cap \mu_2{}^{jk} \tag{D 2}$$

where: $[\mu_r{}^j]_k$ is the result of the $k$-th rule having $j$ as set output for

$j = [VL, L, M, H, VH]$ and $k = [1, 2, 3, \ldots, 25]$;

$\mu_1{}^{jk}$ is the $j$-th component of the first input $\mu_1$ corresponding to the $k$-th rule (e.g., $\mu_1{}^{jk} = \mu_{M,1}$ for $k = 11$);

$\mu_2{}^{jk}$ is the $j$-th component of the second input $\mu_2$ corresponding to the $k$-th rule (e.g., $\mu_2{}^{jk} = \mu_{VL,2}$ for $k = 11$);

The algebraic operation corresponding to the abovementioned Boolean intersection, according to the Mamdani and Zadeh implications, is the minimum value of the two considered components of the five-tuple sets. Thus, Equation D 2 is converted into Equation D 3 as follows:

$$[\mu_r{}^j]_k = \min\left(\mu_1{}^{jk}; \mu_2{}^{jk}\right) \tag{D 3}$$

Since the resulting set will have $n$ elements $j$ within a single component (e.g., rules $r^2$, $r^3$, $r^6$, $r^7$, $r^{11}$ all contribute to component L) the actual member is resolved by means of the Boolean union rule in Equation D 4:

$$\mu_{j,r} = [\mu_r{}^j]_{k,1} \cup [\mu_r{}^j]_{k,2} \cup \ldots \cup [\mu_r{}^j]_{k,n} \tag{D 4}$$

where: $\mu_{j,r}$ is the $j$-th component of the output $\mu_r$;

$n$ is the number of rules $r^k$ having $j$ as result (e.g., $n = 5$ for $j = L$).

The algebraic operation corresponding to the Boolean union operation, according to the Mamdani and Zadeh implications, is the maximum value of the intersections. Thus, Equation D 4 is translated into Equation D 5 as follows:

$$\mu_{j,r} = \max\left( [\mu_r{}^j]_{k,1}; [\mu_r{}^j]_{k,2}; \dots [\mu_r{}^j]_{k,n}\right) \quad \text{(D 5)}$$

Equation D 3 and D 5 were used to determine the components of the resulting five-tuple set $\mu_r = [\mu_{VL,r}; \mu_{L,r}; \mu_{M,r}; \mu_{H,r}; \mu_{VH,r}]$. The five-tuple sets $\mu_i$ were aggregated two-by-two in an iterative process as shown in Figure 13.

*Step 3: Defuzzification*

The defuzzification of the aggregated five-tuples was obtained by using Equation D 6.

$$i_{j,r} = \sum_j q_j \mu_{j,r} \quad \text{(D 6)}$$

where: $i_{j,r}$ represents the defuzzified value of $\mu_{j,r}$;

$q_j$ is the weighting factor of the $j$-th component of the output $\boldsymbol{\mu_r}$;

$\mu_{j,r}$ is the $j$-th component of the output $\boldsymbol{\mu_r}$.

Tesfamaraim and Saatcioglu [22] proposed the $q_j$ factors to be, respectively, $q_{VL} = 0$, $q_L = 0.25$, $q_M = 0.50$, $q_H = 0.75$, and $q_{VH} = 1.00$, however, in the current research, $q_{VL}$ was modified to assume the value of 0.10 so as not to disregard completely the importance of the Very Low risk category.

## Appendix E – Worked Example

A worked example for the calculation of the seismic risk rating is offered in the following appendix. The case of the church of "Santa Maria Maggiore" (Figure E 1) was used for this example (*i* = 61). The church is located in the main square of Alatri, in the diocese of Anagni – Alatri (province of Frosinone, Lazio). It was completed in the $13^{th}$ century and it was built over the ruins of a previous pagan temple dating from the $5^{th}$ century A.D.

*Figure E 1– Church of Santa Maria Maggiore, Alatri, Lazio (Italy).*

### *Seismic Risk Subcomponents*

| | Scenario | Peak ground acceleration, $PGA_i$ [g] | $5^{th}$ percentile [g] | $95^{th}$ percentile [g] | Index of hazard subcomponent, $i_{H,i}$ |
|---|---|---|---|---|---|
| **Hazard** | $T_R$ = 90 years | 0.095 | 0.043 | 0.344 | 0.256 |
| | $T_R$ = 151 years | 0.118 | | | 0.317 |
| | $T_R$ = 1424 years | 0.247 | | | 0.717 |
| | $T_R$ = 2475 years | 0.288 | | | 0.836 |
| **Vulnerabilty** | **Scenario** | | | | **Index of vulnerability subcomponent, $i_{V,i}$** |
| | Minimum | | | | 0.553 |
| | Maximum | | | | 0.622 |
| **Exposure** | **Scenario** | **Occupancy, $p_i$ [people]** | **$5^{th}$ percentile [people]** | **$95^{th}$ percentile [people]** | **Index of occupancy rate, $i_{OR,i}$** |
| | Average occupancy, $p_{av}$ | 57 | 2.05 | 136.20 | 0.420 |
| | Maximum occupancy, $p_{max}$ | 200 | 49.03 | 624.64 | 0.320 |
| | **Scenario** | **Community utilization, $k_i$** | **$5^{th}$ percentile** | **$95^{th}$ percentile** | **Index of community utilization, $i_{CU,i}$** |
| | Regular days, $k_{av}$ | 0.00198 | 0.0016 | 0.193 | 0.010 |
| | Holy day, $k_{max}$ | 0.00692 | 0.015 | 2.368 | 0.006 |
| **Consequences** | **Scenario** | **Equivalent economic value, $V_{eq,i}$ [€]** | **$5^{th}$ percentile [€]** | **$95^{th}$ percentile [€]** | **Index of equivalent economic value, $i_{EEV,i}$** |
| | Minimum | 1,452,461 | 207,225 | 2,656,528 | 0.547 |
| | Maximum | 1,928,546 | | | 0.726 |
| | **Scenario** | **Total score of the church, $Score_i$** | **Maximum possible score** | | **Index of Susceptible Heritage, $i_{SH,i}$** |
| | Susceptible heritage | 38 | 45 | | 0.844 |

*Table E 1 – Indices of risk subcomponent.*

## *Seismic Risk Rating*

### *Via FST*

Step 1: Membership Ratio and Fuzzification of the Inputs

| Indices, $i_i$ | | Fuzzified five-tuple set, $\mu_i$ | Very Low [VL] | Low [L] | Medium [M] | High [H] | Very High [VH] |
|---|---|---|---|---|---|---|---|
| $i_{H,90}$ | 0.277 | $\mu_{H,90}$ | 0 | 0.894 | 0.106 | 0 | 0 |
| $i_{H,151}$ | 0.343 | $\mu_{H,151}$ | 0 | 0.630 | 0.370 | 0 | 0 |
| $i_{H,1424}$ | 0.717 | $\mu_{H,1424}$ | 0 | 0 | 0.134 | 0.866 | 0 |
| $i_{H,2475}$ | 0.836 | $\mu_{H,2475}$ | 0 | 0 | 0 | 0.656 | 0.344 |
| $i_{V,min}$ | 0.553 | $\mu_{V,min}$ | 0 | 0 | 0.787 | 0.213 | 0 |
| $i_{V,max}$ | 0.622 | $\mu_{V,max}$ | 0 | 0 | 0.514 | 0.486 | 0 |
| $i_{OR,AO}$ | 0.420 | $\mu_{OR,AO}$ | 0 | 0.322 | 0.678 | 0 | 0 |
| $i_{OR,MO}$ | 0.320 | $\mu_{OR,MO}$ | 0 | 0.719 | 0.281 | 0 | 0 |
| $i_{CU,RW}$ | 0.010 | $\mu_{CU,RW}$ | 0.959 | 0.041 | 0 | 0 | 0 |
| $i_{CU,HD}$ | 0.006 | $\mu_{CU,HD}$ | 0.975 | 0.025 | 0 | 0 | 0 |
| $i_{EEV,min}$ | 0.499 | $\mu_{EEV,min}$ | 0 | 0.005 | 0.995 | 0 | 0 |
| $i_{EEV,max}$ | 0.649 | $\mu_{EEV,max}$ | 0 | 0 | 0.351 | 0.649 | 0 |
| $i_{SH}$ | 0.844 | $\mu_{SH}$ | 0 | 0 | 0 | 0.622 | 0.378 |

*Table E 2 – Fuzzification of the indices of risk components.*

Step 2: Aggregation of two five-tuple sets

| Input five-tuple sets | | Output five-tuple set | Very Low [VL] | Low [L] | Medium [M] | High [H] | Very High [VH] |
|---|---|---|---|---|---|---|---|
| **Hazard** | | | | | | | |
| $\mu_{H,90}$ | $\mu_{H,151}$ | $\mu_{H,1C}$ | 0 | 0.630 | 0.370 | 0 | 0 |
| $\mu_{H,1C}$ | $\mu_{H,1424}$ | $\mu_{H,1B}$ | 0 | 0 | 0.630 | 0.370 | 0 |
| $\mu_{H,1B}$ | $\mu_{H,2475}$ | $\boldsymbol{\mu_{H}}$ | **0** | **0** | **0** | **0.630** | **0.344** |
| **Vulnerability** | | | | | | | |
| $\mu_{V,min}$ | $\mu_{V,max}$ | $\boldsymbol{\mu_{V}}$ | **0** | **0** | **0.514** | **0.486** | **0** |
| **Exposure** | | | | | | | |
| $\mu_{OR,AO}$ | $\mu_{OR,MO}$ | $\mu_{OR}$ | 0 | 0.322 | 0.678 | 0 | 0 |
| $\mu_{CU,RW}$ | $\mu_{CU,HD}$ | $\mu_{CU}$ | 0.959 | 0.041 | 0 | 0 | 0 |
| $\mu_{CU}$ | $\mu_{OR}$ | $\boldsymbol{\mu_{E}}$ | **0** | **0.678** | **0.041** | **0** | **0** |
| **Consequences** | | | | | | | |
| $\mu_{EEV,min}$ | $\mu_{EEV,max}$ | $\mu_{EEV}$ | 0 | 0 | 0.096 | 0.813 | 0 |
| $\mu_{SH}$ | $\mu_{EEV}$ | $\boldsymbol{\mu_{C}}$ | **0** | **0** | **0** | **0.622** | **0.378** |

*Table E 3 – Aggregation from seismic risk subcomponents to seismic risk components (bolded).*

| Input five-tuple sets | | Output five-tuple set | Very Low [VL] | Low [L] | Medium [M] | High [H] | Very High [VH] |
|---|---|---|---|---|---|---|---|
| $\mu_{E}$ | $\mu_{C}$ | $\mu_{EC}$ | 0 | 0 | 0.622 | 0.378 | 0 |
| $\mu_{EC}$ | $\mu_{V}$ | $\mu_{VEC}$ | 0 | 0 | 0.514 | 0.486 | 0 |
| $\mu_{VEC}$ | $\mu_{H}$ | $\boldsymbol{\mu_{R}}$ | **0** | **0** | **0** | **0.514** | **0.344** |

*Table E 4 – Aggregation from seismic risk components to seismic risk (bolded).*

Step 3: Defuzzification

| | Aggregated five-tuple set, $\mu_i$ | Indices of seismic risk component, $i_i$ | |
|---|---|---|---|
| Hazard | $\mu_H$ = [0; 0; 0; 0.630; 0.344] | $i_H$ | 0.816 |
| Vulnerability | $\mu_V$ = [0; 0; 0.514; 0.486; 0] | $i_V$ | 0.622 |
| Exposure | $\mu_E$ = [0; 0.678; 0.041; 0; 0] | $i_E$ | 0.190 |
| Consequences | $\mu_C$ = [0; 0; 0; 0.622; 0.378] | $i_C$ | 0.844 |

*Table E 5 – Defuzzification of the seismic risk component into indices.*

| | Aggregated five-tuple set, $\mu_i$ | Seismic risk rating, $i_i$ | |
|---|---|---|---|
| Seismic Risk | $\mu_R$ = [0; 0; 0; 0.514; 0.344] | $i_R$ | 0.730 |

*Table E 6 – Defuzzification of the seismic risk into rating.*

*Via multilinear regression equations*

| | Indices of seismic risk subcomponent, $i_i$ | | Indices of seismic risk rating | |
|---|---|---|---|---|
| Hazard | $i_{H,90}$ | 0.277 | $i_H$ | 0.669 |
| | $i_{H,151}$ | 0.343 | | |
| | $i_{H,1424}$ | 0.717 | | |
| | $i_{H,2475}$ | 0.836 | | |
| *Vulnerability* | $i_{V,min}$ | 0.553 | $i_V$ | 0.612 |
| | $i_{V,max}$ | 0.622 | | |
| *Exposure* | $i_{OR,AO}$ | 0.420 | $i_E$ | 0.183 |
| | $i_{OR,MO}$ | 0.320 | | |
| | $i_{CU,RW}$ | 0.010 | | |
| | $i_{CU,HD}$ | 0.006 | | |
| *Consequences* | $i_{EEV,min}$ | 0.547 | $i_C$ | 0.500 |
| | $i_{EEV,max}$ | 0.726 | | |
| | $i_{SH}$ | 0.844 | | |

*Table E 7 – Determination of the indices of seismic risk components via Equations 12 through 15.*

| | Indices of seismic risk component, $i_i$ | | | Seismic risk rating, $i_i$ | | |
|---|---|---|---|---|---|---|
| | | From Table E 5 | From Table E 6 | | From Table E 5 values | From Table E 6 values |
| Seismic risk | $i_H$ | 0.816 | 0.669 | $i_R$ | 0.654 | 0.569 |
| | $i_V$ | 0.622 | 0.612 | | | |
| | $i_E$ | 0.190 | 0.183 | | | |
| | $i_C$ | 0.844 | 0.500 | | | |

*Table E 8 – Determination of the seismic risk rating via Equation 16.*